

# CFD Analysis of a Flocculation Tank and Design Recommendations

**By: Yong Sheng Khoo**

**Jesse Prager**

## Abstract

A flocculation tank purifies contaminated water by mixing in a solution that precipitates out flocs. Little information is available about the fluid behavior within the flocculation tank. The flow is in turbulent regime and involves separation, reattachment and high shear. By analyzing the flocculation tank using the k- $\epsilon$  realizable model in FLUENT, the fluid behavior has been characterized, and various geometrical configurations have been simulated. The results of our experimental will be instrumental to AguaClara's design team which produces designs for hydraulic water treatment plants installed in Honduras.

The fluid behavior has been analyzed by examining the uniformity of the energy dissipation rate ( $\epsilon$ ) within the flocculation tank, and by determining performance parameters which relate to the formation and break up of flocs. The uniformity of  $\epsilon$ , indicates that there is high mixing throughout the entire flocculation tank. The uniformity of the flocculation tank is gauged by visual plots of  $\epsilon$ , and a pdf quantifying the distribution of flocculation area within  $\epsilon$  ranges. Performance parameters are derived using dimensional analysis, and relate  $\epsilon$  to the relative velocity within the viscous and non-viscous sub-regions, and to the shear stress exerted on a particle in drag. The performance parameters are  $\epsilon$  raised to various powers multiplied by the residence time, and are found by summing the time-averaged cell values using FLUENT UDF scripts.

The result of the research indicates that the optimal flocculation tank design in terms of uniformity occurs at a flocculation tank height of .3 m, baffle width of .1 m and clearance height of .1 m. The optimal flocculation tank design in terms of the performance parameters occurs at a flocculation tank height .2 m, baffle width of .1 m and a clearance height of .1 m. The flocculation tank analyzed at  $Re=10,000$  is somewhat sensitive to Reynolds number, while the flocculation tank performance is not sensitive to the turbulent boundary inlet condition. Overall the design of the flocculation tank produced reasonable results which match expected results of hydraulic flocculation tanks found in literature.

The results of the report suggest that a smaller flocculation tank height with intersecting energy dissipation regions will produce the greatest formation of flocs per area.

## **I. Introduction**

In order to better understand the behavior of the fluid in the flocculation tank, the CFD simulation team has modeled the tank using FLUENT. This approach allows the analysis of different geometries, flows and boundary conditions without the difficulty of setting each of these cases up in an experimental lab. The results produced by the simulation enables examining detailed profiles of velocity, turbulence energy dissipation, turbulent kinetic energy, and any derived parameter in terms of these variables. This semester our main goals have been to optimize the flocculation tank design, and understand how the region of turbulent energy production and dissipation over each baffle interact. Research of the flocculation tank using these advanced tools improves the performance of the flocculation tank, and can lead to smaller more cost effective designs.

## **II. Procedures**

### **II.1 Geometry of Flocculation Tank**

There are a few important parameters of flocculation tank that will affect the flow properties in the flocculation tank. The important parameters are number of baffles turning ( $N$ ), baffle spacing ( $bs$ ), flocculation tank height ( $fh$ ), and baffle clearance height ( $ch$ ). To make sure that the flow properties are not affected by the inlet and outlet boundary conditions, we want  $N$  to be large. However, large  $N$  will contribute to long computational time. So to balanced both factor,  $N$  of 5 was chosen as the number of baffle turning. Knowing the general geometry of the flocculation tank, we can now focus our analysis on the geometry that we are interested.

### **II.2 Gambit and FLUENT**

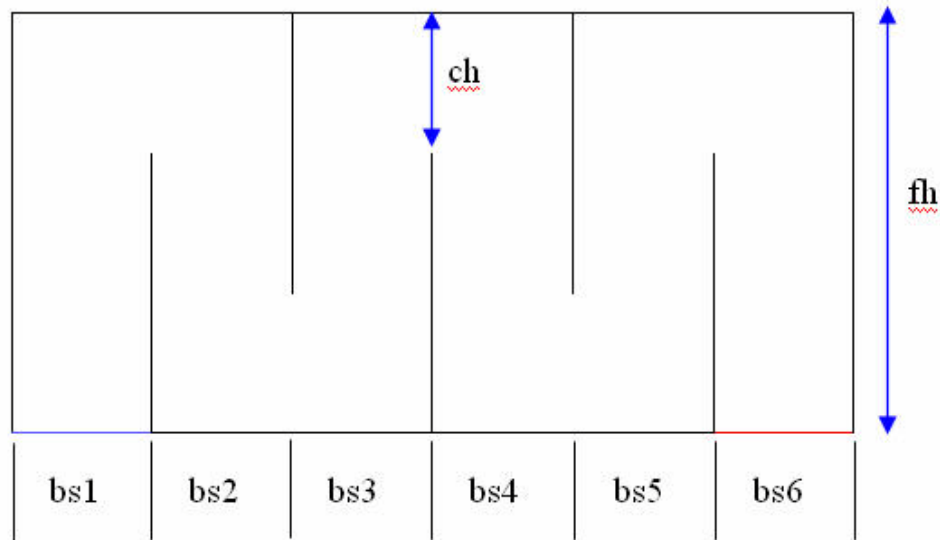
#### **II.2.1 Automation of Mesh Creation**

For this research project, flocculation tank with different geometric properties were evaluated. In order to prevent the tedious process of generating mesh from scratch, journal script for automating the mesh creation process were used.

In general, every time we use Gambit for creating mesh, it logs every single action that we do into a journal file. This journal file is very useful as it enables the user to troubleshoot the code if problems arise.

By changing the appropriate geometry parameters of the journal files into variables, we are able to create mesh with different geometries by changing the value of the variables.

Refer to Appendix A-1 for script files for the automation mesh creation of flocculation tank with 5 baffles turning.



Legend:

bs = baffle spacing

ch = clearance height

fh = flocculation tank height

Figure II.1. Flocculation tank geometry parameters

Using the [script](#) provided, users can investigate the necessary geometry by just changing the parameter of baffle spacing, clearance height and flocculation tank height as illustrated in figure II.1. Upon changing those parameter, users just have to run the script in Gambit and the finalized mesh is ready for implementation in FLUENT.

Similarly, a script in FLUENT can process a completed mesh, and automatically set up the solver, initial conditions, fluid properties, convergence criteria, and save the convergence solution data file to be analyzed later. Please refer to Appendix A-2 for the script.

## Modifying the Journal File

Following is the sample of the heading of the journal file that was added to declare the value of different parameters.

```
/clearance height  
$ch = 0.1
```

```
/floculator height  
$fh = 0.5
```

```
/create baffle spacing  
$bs1 = 0.1
```

```
/create x-coordinate  
$w0 = 0  
$b1 = $w0+$bs1
```

```
/create y-coordinate  
$y1 = $ch  
$y2 = $fh-$ch
```

Note that '/' means commenting on the code.

Note also that the parameters are initialized to  $ch = 0.1$ ,  $fh = 0.5$ ,  $bs = 0.1$ .

Note also that a '\$' is added in front of those parameters to denote them as variables in Gambit.

Note also Gambit recognize mathematical operators.

By relating different coordinates of the flocculation tank to the declared parameters, we can generate meshes with different geometry by just changing the heading of the journal file.

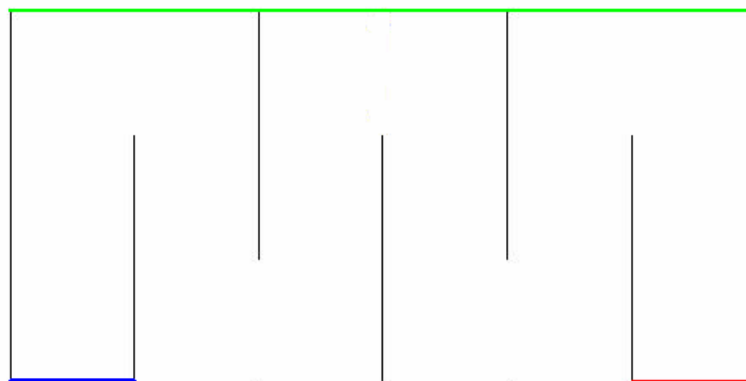
Look at the Appendix A-1 for the complete script.

## II.2.2 Setting up Problem in FLUENT

With mesh created, we can now use FLUENT to set up the problem. Following steps illustrate what is needed to be done.

1. Import generated mesh file
2. Define turbulence model
  - Different turbulence model are appropriate for different flow properties
  - K- $\epsilon$  realizable model is chosen for the flow in flocculation tank (further discussed in later section)
3. Define materials (liquid water for our case)
4. Define operating conditions (use default operating pressure)
5. Define boundary conditions (Details below)
6. Set control solution
  - Select second order discretization method instead of first order method
7. Initialize the problem with the inlet properties
8. Set Residual to 1e-05
  - The residual is a measure of how well the current solution satisfies the discrete form of each governing equation
9. Solve the problem by iterating

### Defining Boundary Conditions



- Top (Exposed to air)
- Wall
- Outlet
- Inlet

Figure II.2. Boundary conditions of flocculation tank

Figure II.2 shows the boundary conditions of the flocculation tank. The top part of the flocculation is open, so a symmetry boundary conditions is employed. The inlet boundary condition is set to inlet velocity of 0.1 m/s, and the outlet is set to pressure outlet.

**Table II.1. Boundary conditions**

**Boundary Boundary Conditions**

Top	Symmetry
Wall	Wall
Inlet	Velocity Inlet (0.1m/s)
Outlet	Pressure Outlet

**II.3 Validation of Turbulence Models**

**Turbulence Modeling Resolution Problem**

Computational Fluid Dynamics works by iteratively changing the values of the variables to reduces the residuals, or errors of the governing equation. The governing equations in our model is conservation of mass and conservation of momentum as shown below in Eq. 1 and Eq. 2:

$$\frac{\partial u}{\partial x} + \frac{\partial v}{\partial y} + \frac{\partial w}{\partial z} = 0$$

**Equation 1. Conservation of Mass**

$$\rho \left( \overbrace{\frac{\partial \mathbf{v}}{\partial t} + \mathbf{v} \cdot \nabla \mathbf{v}}^{\text{Inertia}} \right) = \underbrace{-\nabla p}_{\text{Pressure gradient}} + \underbrace{\mu \nabla^2 \mathbf{v}}_{\text{Viscosity}} + \underbrace{\mathbf{f}}_{\text{Other forces}}$$

$$\rho \left( \frac{\partial u}{\partial t} + u \frac{\partial u}{\partial x} + v \frac{\partial u}{\partial y} + w \frac{\partial u}{\partial z} \right) = -\frac{\partial p}{\partial x} + \mu \left( \frac{\partial^2 u}{\partial x^2} + \frac{\partial^2 u}{\partial y^2} + \frac{\partial^2 u}{\partial z^2} \right) + \rho g_x$$

**Equation 2. Conservation of Momentum**

The conservation of Momentum equation can be simplified to Reynolds Averaged Navier Stokes Equation (for x,y directions) in Eq. 3 by estimating velocity and pressure in terms of mean value (u) and fluctuation (u') and averaging all terms as shown below:

$$\frac{\partial \bar{u}_i}{\partial t} + \frac{\partial \bar{u}_j \bar{u}_i}{\partial x_j} = \bar{f}_i - \frac{1}{\rho} \frac{\partial \bar{p}}{\partial x_i} + \nu \frac{\partial^2 \bar{u}_i}{\partial x_j \partial x_j} - \frac{\partial \overline{u'_i u'_j}}{\partial x_j}$$

### Equation 3. Reynolds Averaged Navier Stokes Equation

With the conservation of mass equation, and conservation of momentum equations in the x and y direction, there are three governing equations. However with the introduction of the velocity fluctuation variable (u',v'), as shown above there are four variables (u,v,u',v',p). Thus, the problem becomes unresolvable unless additional equations are formulated to relate the variables. This is the **Turbulence Modeling Resolution Problem**.

The k-epsilon model overcomes this problem by relating the product of the velocity fluctuation terms to gradients of the mean velocity.

$$-\overline{u'_i u'_j} = \nu_t \left( \frac{\partial \bar{U}_j}{\partial x_i} + \frac{\partial \bar{U}_i}{\partial x_j} \right)$$

The  $\nu_t$  represents a variable which can be related to the turbulent kinetic energy (k) and the energy dissipation rate ( $\epsilon$ ).

$$\nu_t = c_\mu \frac{k}{\epsilon}$$

The turbulent kinetic energy (k) and energy dissipation rate ( $\epsilon$ ) are governed by the following equations.

For turbulent kinetic energy  $k$

$$\frac{\partial}{\partial t}(\rho k) + \frac{\partial}{\partial x_i}(\rho k u_i) = \frac{\partial}{\partial x_j} \left[ \left( \mu + \frac{\mu_t}{\sigma_k} \right) \frac{\partial k}{\partial x_j} \right] + P_k + P_b - \rho \epsilon - Y_M + S_k$$

For dissipation  $\epsilon$

$$\frac{\partial}{\partial t}(\rho \epsilon) + \frac{\partial}{\partial x_i}(\rho \epsilon u_i) = \frac{\partial}{\partial x_j} \left[ \left( \mu + \frac{\mu_t}{\sigma_\epsilon} \right) \frac{\partial \epsilon}{\partial x_j} \right] + C_{1\epsilon} \frac{\epsilon}{k} (P_k + C_{3\epsilon} P_b) - C_{2\epsilon} \rho \frac{\epsilon^2}{k} + S_\epsilon$$

Thus, these definitions of k and  $\epsilon$  enable the system to be fully resolvable with 6 variables (u,v,p, $\nu_t$ ,k, $\epsilon$ ) and 6 equations.



The k- $\epsilon$  model is one approach to create a resolvable problem and many other methods have been formulated. Certain models solve particular types of problem better, therefore it is necessary to gauge the performance of the turbulence models using a similar example.

### Comparing Turbulence Models Using Back-step Example

To determine on the turbulence model to use, a flow over back-step was compared with the literature experimental data. Figure II.3 shows the flow of  $Re = 48000$  over the channel. In the middle of the channel, the flow separate due to the small step size of height  $h$ . The flow reattaches at about 7 times the step height further downstream. This flow property is similar to the 180 degree bend in the flocculation tank where we have flow separation and reattachment downstream (Figure II.4).

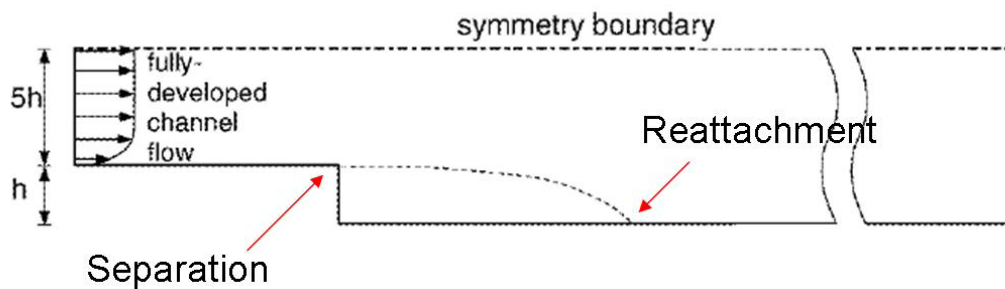


**Figure II.3. Flow over backstep in a open channel ( $Re = 48000$ , Reattachment length =  $7h$ )**

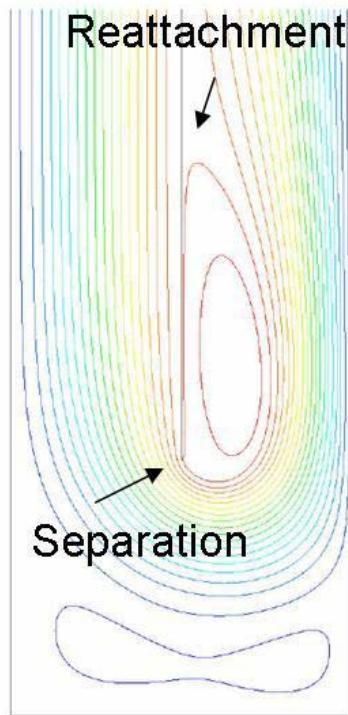


**Figure II.4. Flow over 180 degree turn in flocculation tank**

The back step flow was analyzed using K- $\epsilon$ , K- $\omega$  SST, K- $\epsilon$  realizable, K- $\epsilon$  RNG, RSM turbulence models. The reattachment points of all the turbulence models was determined so that the reattachment ratio could be compared with the experimental data.

Plotting the derivative  $du/dy$ , the change in direction of velocity in x direction with respect to y at the wall, the reattachment point is easily identified. At the wall, separated flow will give a negative  $du/dy$ , while reattaches flow has a positive  $du/dy$  value. Figure II.5 shows the derivative of  $du/dy$  vs x direction for different turbulence models.

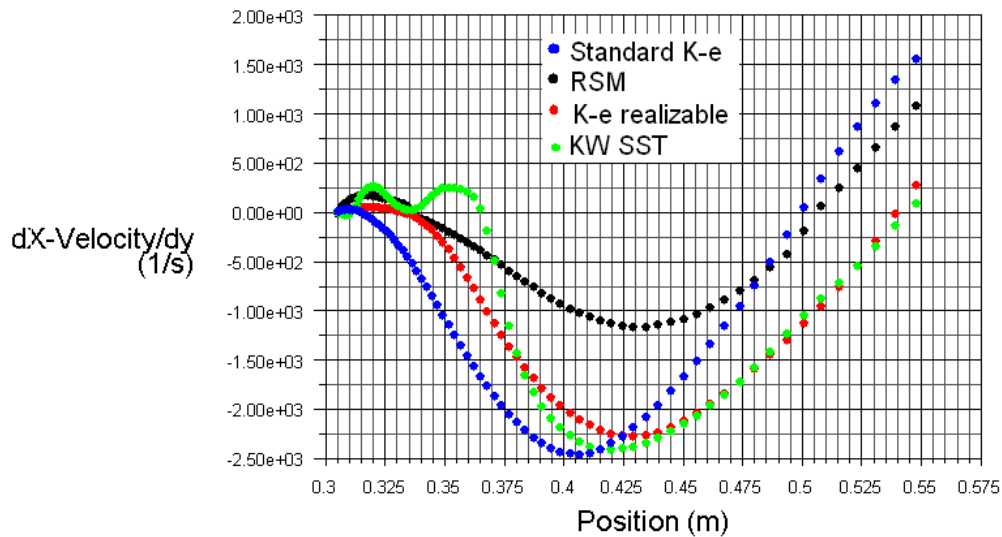


**Figure II.5.  $dU/dy$  for Different Turbulence Models**

**Table II.2. Reattachment ratio with different turbulence models**

Turbulence Model	K-e	K-W SST	K-e realizable	RSM
Reattachment Ratio	$0.195/0.038 = 5.13$	$0.242/0.038 = 6.37$	$0.235/0.038 = 6.18$	$0.2/0.038 = 5.26$

From table II.2, the K- $\epsilon$  model under-predicts the reattachment length, as known by most literature. K- $\omega$  SST and K- $\epsilon$  realizable gives the most accurate representation of the back step flow with reattachment length of 6.37 and 6.18. However, from literature reviews, K- $\epsilon$  realizable is more proven for a variety of types of flows. Thus K- $\epsilon$  realizable has been chosen as the model for flow in the flocculation tank. Below in Figure II.6, the stream contours (of the averaged velocity) with  $Re=48,000$  for the k- $\epsilon$  realizable model case closely approximate the experimental results.

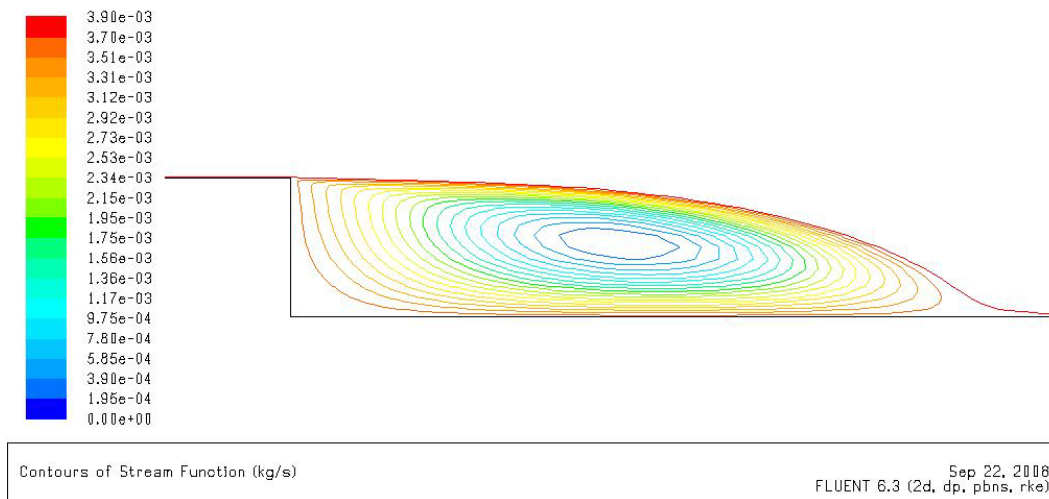


**Figure II.6. Flow over backstep using K-e realizable model**

## II.4 UDF

Following the converged solution in FLUENT, data needs to be extracted from the cells. This is accomplished by using a User Defined Function (UDF). UDFs can be called upon to cycle through all of the cells, and sum relevant parameters based on the corresponding values of variables in the cell. The structure of UDFs used to determine relevant parameters in the program were structured as follows:

- Declaration of DEFINE macro: defines when the function is called  
`DEFINE_ON_DEMAND(on_demand2_calc)`
- Variable declarations: defines structure, variables, and parameters
 

```

Domain *d;      double pos_x;      int density=1000;
Thread *t;      double pos_y;      double visc=1e-6;
cell_t c;       double sum=0;
Node *nod;
      
```
- Loops over cells
 

```

thread_loop_c(t,d)
{
    begin_c_loop(c,t)
    {
      
```
- Meat of the Code: makes reference to
 

```

C_D(c,t)        turb kin energy dissipation
NODE_X(nod)     node x-position
    }
      
```

- }  
□ Print Results to Screen: uses *printf* to display results

The UDF used for this semester are available on the wiki, and follow the above format.

## II.5 Analyzing Results

### II.5.1 Based on Performance Parameters

Given the converged solution, how does one determine whether one design is more optimal than another? The optimality is based on the mechanism of the formation of floc particles, as well as the break up of flocs. The formation of flocs is directly related to the relative velocity of the particles in the flocculator. In the viscous sub-range, the relative velocity of the particles is proportional to the velocity gradient ( $G$ ). The velocity gradient in the viscous subregion is  $\sqrt{\epsilon/\nu}$ , and the relative velocity is proportional to  $\epsilon^{1/2}$ . This behavior only occurs in the first stage of flocculation, while the majority of the flocculation is done in larger length scales, above the Kolmogorov length scale. Here the relative velocity is proportional to the  $\epsilon^{1/3}$ . The floc break-up is directly related to the shear stress applied by the fluid on the floc particle. For all length scale, this is proportional to the turbulent energy dissipation rate ( $\epsilon$ ).

Also, important to both the break up, and formation of flocs is the residence time of the particle ( $\theta$ ). Multiplying the residence time of the particle with each of the above parameters creates performance parameters for formation of flocs,  $G\theta$ ,  $\epsilon^{1/2}\theta$ , and  $\epsilon^{1/3}\theta$ , and break up of flocs,  $\epsilon\theta$ . These quantities can be determined for the entire flocculator by summing up the value of each cell normalized by the volume flow rate. This is accomplished by using the UDFs, as defined above. The formulation of the summed quantity is solved for using the  $G\theta$  quantity below. By a similar process, the performance parameters of the other quantities equals  $1/Q*\Sigma(G, \epsilon^{1/2}, \epsilon^{1/3})*(cell\_area)$ .

$$G\theta_{baffle} = \frac{1}{Q} \sum_{fe} G_{fe} \theta_{fe} Q_{fe}$$

$$\theta_{fe} = \frac{\nabla_{fe}}{Q_{fe}} = \frac{\Delta x \Delta y}{|v_x \Delta y| + |v_y \Delta x|}$$

$$G\theta_{baffle} = \frac{1}{Q} \sum_{fe} G_{fe} \nabla_{fe}$$

$$G_{fe} \propto \sqrt{\frac{\epsilon_{fe}}{\nu}}$$

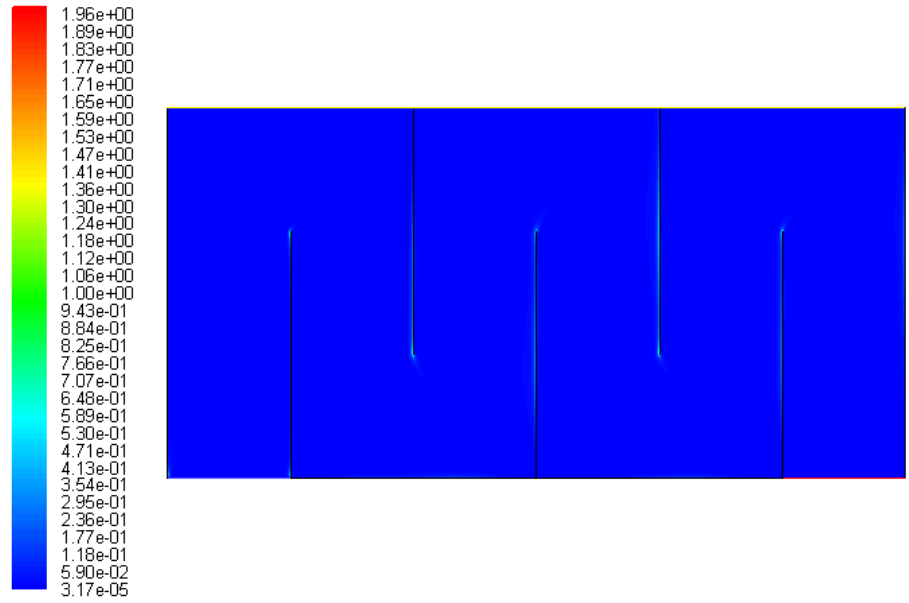
$$G\theta_{baffle} = \frac{1}{Q} \sum_{fe} \sqrt{\frac{\epsilon_{fe}}{\nu}} \nabla_{fe}$$

$$G\theta_{baffle} = \frac{1}{Q\sqrt{\nu}} \sum_{fe} \epsilon_{fe}^{1/2} \nabla_{fe}$$

**Figure II.7. Performance Parameter Formulation**

## II.5.2 Based on Uniformity of Flocculation Tank Energy Dissipation

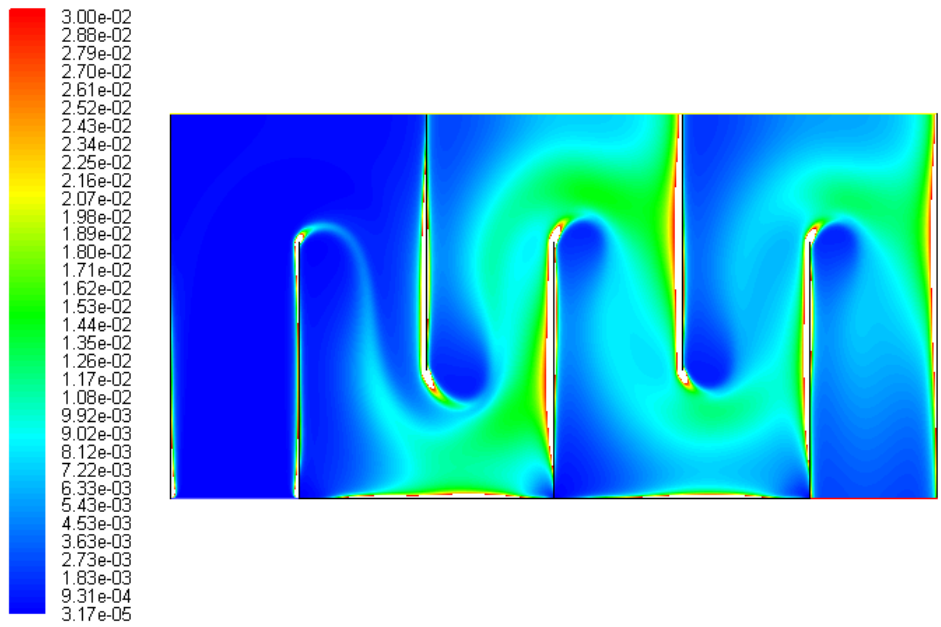
From above discussion, it was known that energy dissipation rate play a big role in determining the performance of the flocculation tank. At the beginning of the flocculation, flocs collision is due to viscous effect. The performance parameter at the beginning is a function of  $\epsilon^{1/2}$ . For the rest of the flocculation, flocs collision is due to  $\epsilon^{1/3}$ . Since energy dissipation rate plays an important role in particle collision, determining the uniformity of the energy dissipation rate would be a good choice. The first approach of determining uniformity was to plot the contour of energy dissipation rate in FLUENT and determining the uniformity by visual inspection. Since the range of energy dissipation rate is very large with most of the energy dissipation rate concentrated at the smaller scale, we need to reduce the energy dissipation rate to the appropriate range that we are interested in.



Contours of Turbulent Dissipation Rate (Epsilon) (m2/s3)

Dec 11, 2008  
FLUENT 6.3 (2d, dp, pbns, rke)

**Figure II.8. Energy Dissipation Rate without ranging**



Contours of Turbulent Dissipation Rate (Epsilon) (m2/s3)

Dec 11, 2008  
FLUENT 6.3 (2d, dp, pbns, rke)

**Figure II.9. Energy Dissipation Rate with ranging**

Figure II.8 and II.9 shows the comparison of the energy dissipation plot with and without adding the range. As can be seen, setting the appropriate range of energy dissipation rate enables us to better visualize the contour of energy dissipation rate.

Using this visual method, we can indeed evaluate the uniformity of the energy dissipation rate. A less subjective and powerful way of determining the uniformity of energy dissipation rate is to use the UDF to collect the individual cell data and plot out the energy dissipation distribution of the flocculation tank. To plot the distribution, separate the range of the energy dissipation rate into different bins. The area with different energy dissipation rate is then captured into the appropriate bins for analysis. Plotting the energy dissipation rate against fractional area will give us the distribution that we are interested.

### **III. Results & Discussion**

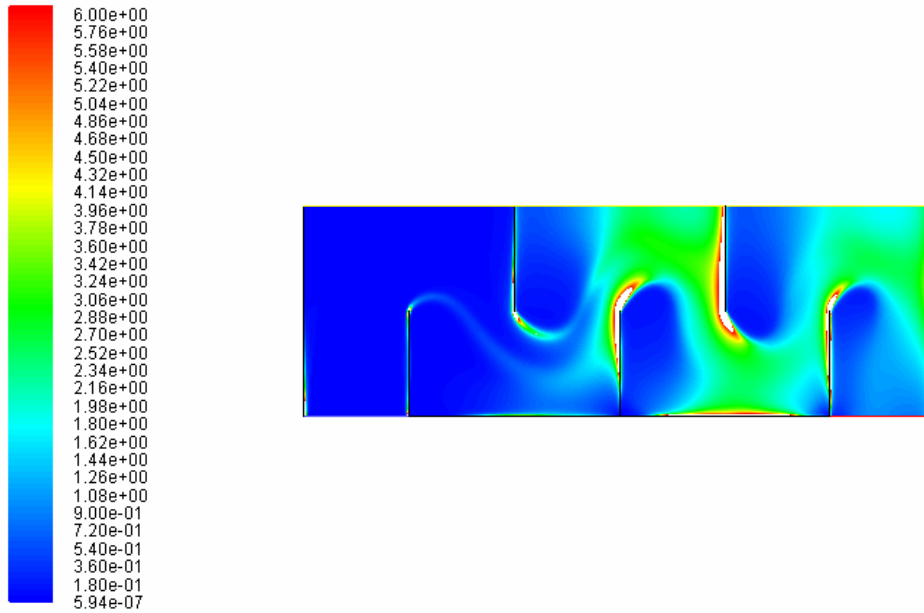
#### **Result 3.1: Uniform Energy Dissipation Rate Approach in Determining Optimal Geometry**

One way to determine the optimal geometry is by evaluating the uniformity of energy dissipation rate. Since energy dissipation rate is the core parameter that influence the particle collision, it is reasonable to assume that uniform energy dissipation rate will give a better performing flocculation tank.

Different geometric space was explored to determine flocculation tank with uniform energy dissipation rate. The optimization method utilized started with an initial geometry. From the initial geometry, we then changed the geometry parameters such as clearance height, baffle spacing and flocculation tank height. If changes in geometry resulted in a more uniform energy dissipation rate than the initial geometry, the new geometry is called the incumbent.

Following this process, geometries were investigated in all possible geometric space. At the end of the investigation, the final incumbent will be chosen as the optimal solution.





Contours of normalized-epsilon

Dec 08, 2008  
 FLUENT 6.3 (2d, dp, pbns, rke)

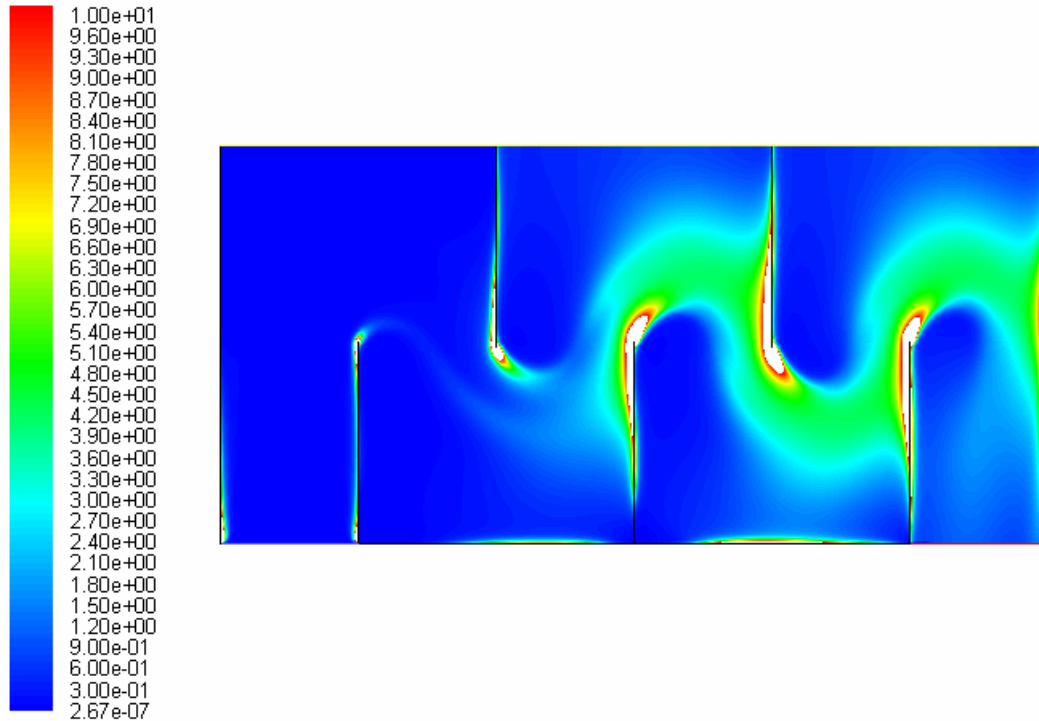
**Figure III.1. Turbulent Dissipation Rate ( $fh = 2b$   $bs = 0.1$   $ch = 1b$ )**

### Getting Started with an Initial Geometry

From first semester, we concluded that clearance height should be no smaller than the baffle spacing. We would also like to start our investigation of the geometric space by having the most overlapping energy dissipation region. Employing the two constraints, we come up with the initial flocculation tank height of  $2b$ . Figure III.1 shows the contour of turbulent dissipation rate with such geometry. We see that the energy dissipation rate is fairly uniform. Since this is our starting geometry, there is no other geometry to compare with. So this will be the new incumbent.

### Baffle Spacing Investigation

From initial geometry in figure III.1, we see that there is large blue region in the inner turn. By reducing the baffle spacing we hope to reduce the non-active region.



Contours of normalize-epsilon

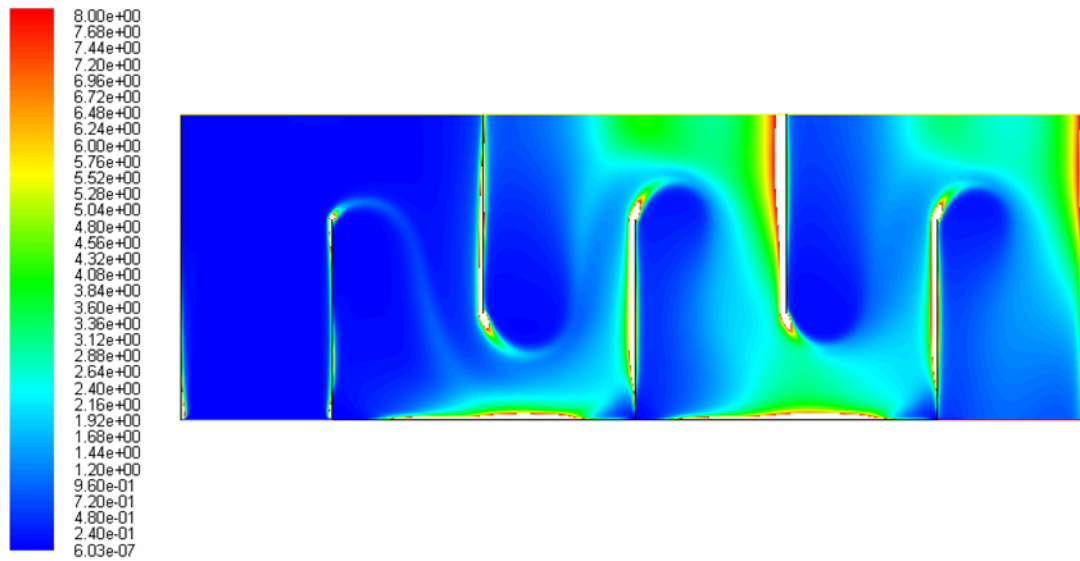
Dec 08, 2008  
 FLUENT 6.3 (2d, dp, pbns, rke)

**Figure III.2. Turbulent Dissipation Rate ( $fh = 0.2$   $bs = 0.07$   $ch = 0.1$ )**

Reducing the baffle spacing does not give the desired effect, and we do not have a new incumbent. Since the uniformity decreases, this is not the right parameter to change.

### Clearance Height Investigation

Another geometric space that we can investigate is the clearance height. Though it was recommended from previous semester that clearance height of one baffle spacing is optimal for the design for one baffle turn, it would be interesting if we observe different results for multiple baffles turning.



Contours of normalized-epsilon

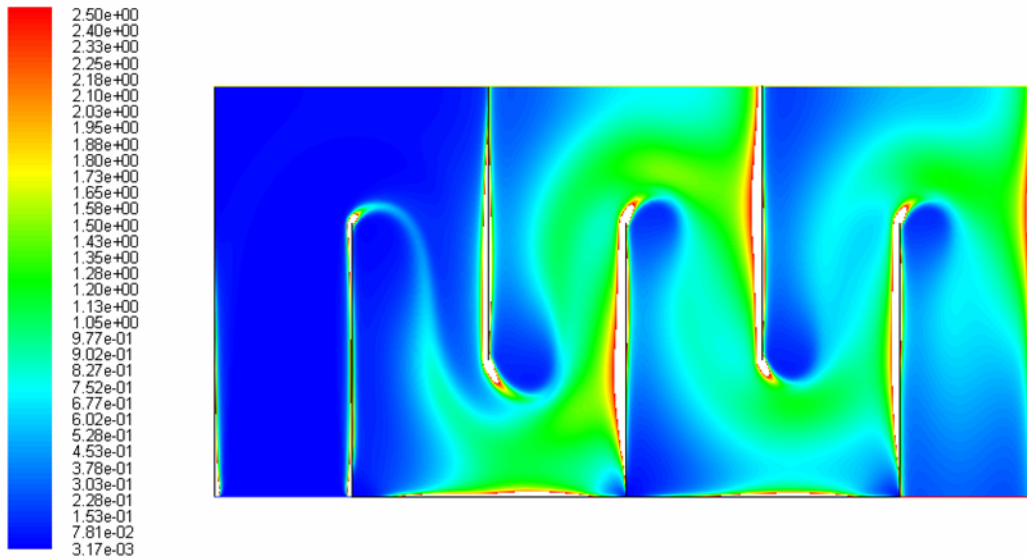
Dec 08, 2008  
 FLUENT 6.3 (2d, dp, pbns, rke)

**Figure III.3. Turbulent Dissipation Rate ( $fh = 2b$   $bs = 0.1$   $ch = 0.7b$ )**

Changing clearance height parameter also did not give desirable result. Decrease in clearance height create a constriction of the flow and we have very high energy dissipation rate in that region. The result observed is the same as of last semester's result of one baffle turning. Changing clearance height geometric space will not give us a better result.

### **Flocculation Tank Height Investigation**

Having investigated two of the three parameters, we are left with final parameter, which is the flocculation tank height. Flocculation tank height of  $2b$  might be providing too much overlapping region. Reducing overlapping of the tail of the energy dissipation region might give a more uniform distribution.

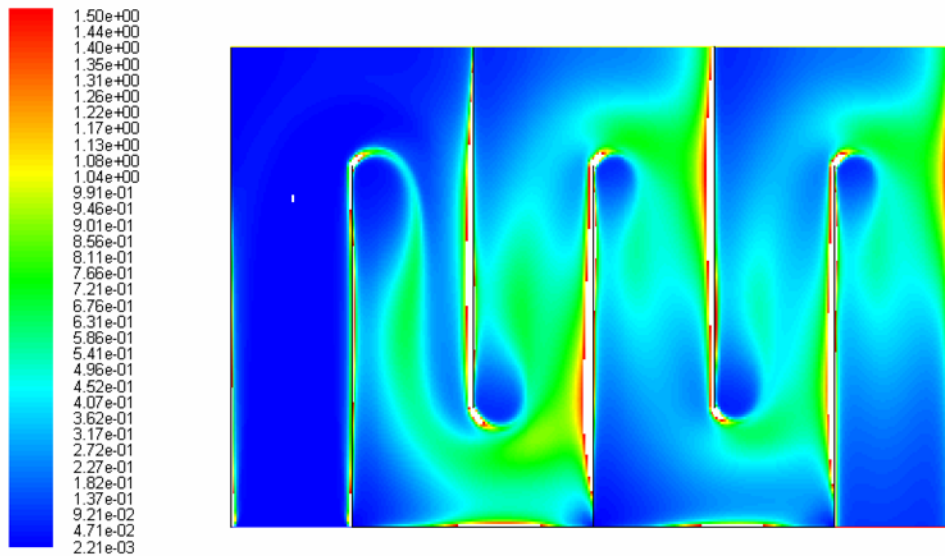


Contours of normalized-epsilon

Dec 08, 2008  
FLUENT 6.3 (2d, dp, pbns, rke)

**Figure III.4. Turbulent Dissipation Rate ( $fh = 3b$   $bs = 0.1$   $ch = 1b$ )**

Figure III.4 shows the longer flocculation tank height of  $3b$ . This geometry give us a more uniform energy dissipation rate than the previous incumbent (Figure 1). This geometry configuration will be the new incumbent. Since changing this geometric space give desirable result, further investigation into this parameter is needed.



Contours of normalized-epsilon

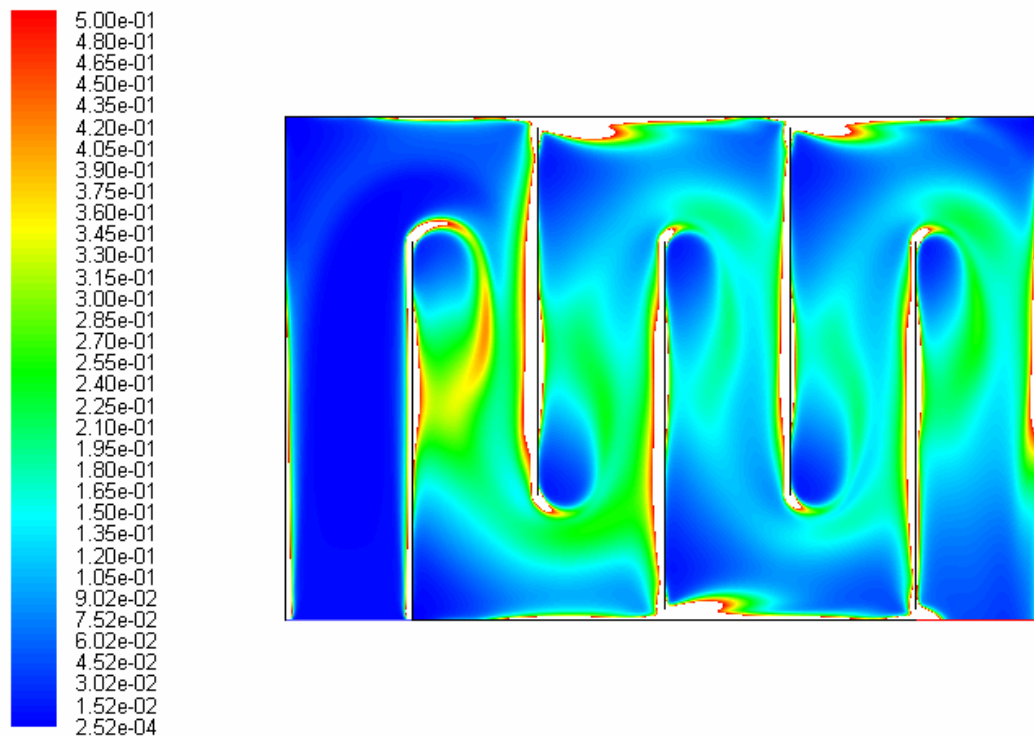
Dec 08, 2008  
FLUENT 6.3 (2d, dp, pbns, rke)

**Figure III.5. Turbulent Dissipation Rate ( $fh = 0.4$   $bs = 0.1$   $ch = 0.1$ )**

Comparing figure 4 and 5, we see that flocculation tank height of 4b does not give a more uniform energy dissipation rate. Therefore, flocculation tank height of 3b is still the incumbent.

### Adding of Slots Investigation

Notice that there is a region of low energy dissipation rate right before the turning. Another interesting geometric space that might be worth investigating is to add a small slot at the baffle so that water can flow directly through the baffles. The hope is that this method will reduce the stagnant region.



Contours of normalized-epsilon

Dec 08, 2008  
FLUENT 6.3 (2d, dp, pbns, rke)

**Figure III.6. Turbulent Dissipation Rate ( $f_h = 0.4$   $b_s = 0.1$   $ch = 0.1$   $slot = 0.1b$ )**

From figure III.6, we see that adding small slots at the bottom of baffles does not give us the desired result. The small slot causes the water to flow directly through them and the constriction effect of the flow causes undesirably high energy dissipation rate region.

After considering all possible geometric space, we concluded that the optimal geometry for flocculation tank is  $f_h = 3b$ ,  $b = 0.1$ ,  $ch = 1b$  as seen in figure III.4.

### Result 3.2: Complementary Solution to Analysis of Energy Dissipation Distribution

From section 3.1, we concluded the uniformity of energy dissipation rate using visual investigation. This section presents the results using a statistical method to complement the result from previous section.

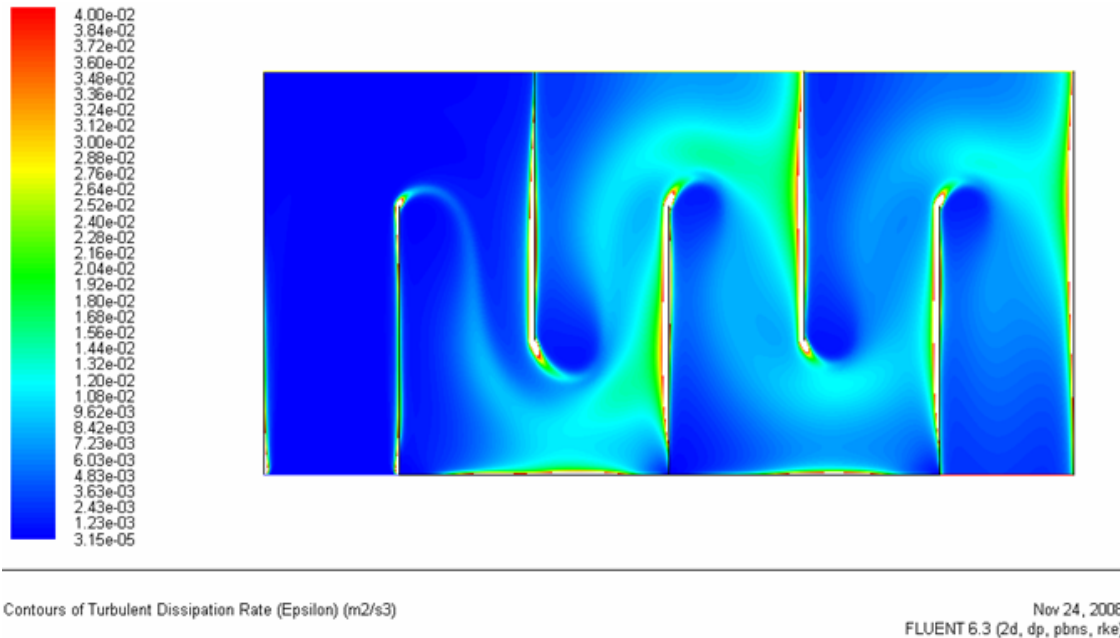
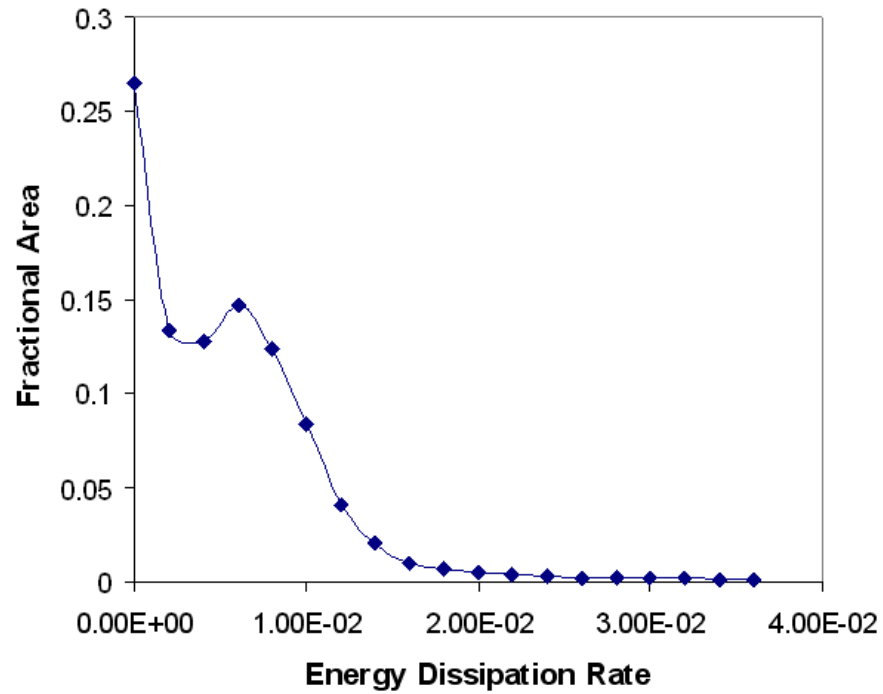


Figure III.7. Contour of Energy Dissipation Rate ( $h/b=3$ )

Figure III.7 shows the contour of the energy dissipation rate. Visually, we can judge the uniformity of the energy dissipation rate for the given geometry. A less subjective way of characterizing the uniformity of the energy dissipation rate is to use UDF to analyze and plot out the distribution of the energy dissipation rate. Appendix B-1 shows the UDF script.

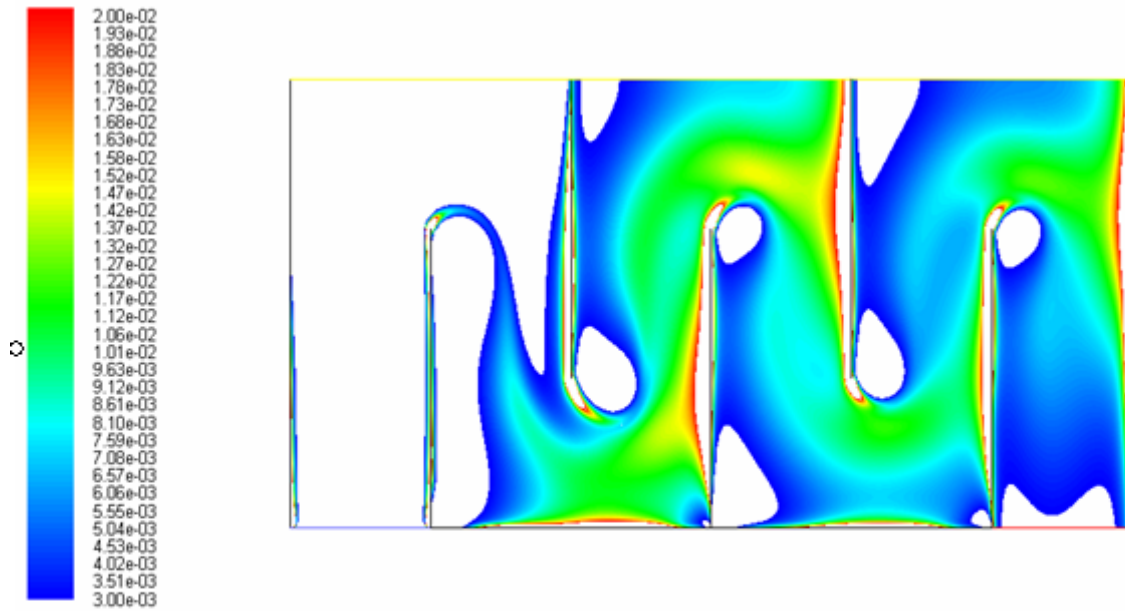
### Energy Dissipation Rate Distribution



**Figure III.8. Distribution of Energy Dissipation Rate ( $h/b=3$ ) with "hump"**

Figure III.8 shows the distribution of the energy dissipation. Note that there is a hump in the distribution. The peak of the hump is around energy dissipation rate of 0.006  $m^2/s^3$ . There might be relationship between the hump and the uniformity of the energy dissipation rate.

Smaller range of energy dissipation rate was set to investigate this relationship.



Contours of Turbulent Dissipation Rate (Epsilon) (m2/s3)

Nov 24, 2008  
FLUENT 6.3 (2d, dp, pbns, rke)

**Figure III.9. Contour of Energy Dissipation Rate ( $h/b=3$ ) with Tighter Range**

From figure III.9, setting a tighter range of energy dissipation rate, we see that the contour is dominated by the blue and green region which is from the range of 0.005 to 0.01 m<sup>2</sup>/s<sup>3</sup>. This explains the appearance of hump in figure 2.

To further investigate this phenomena, another flocculation geometry with flocculation tank height of 4b is plotted.



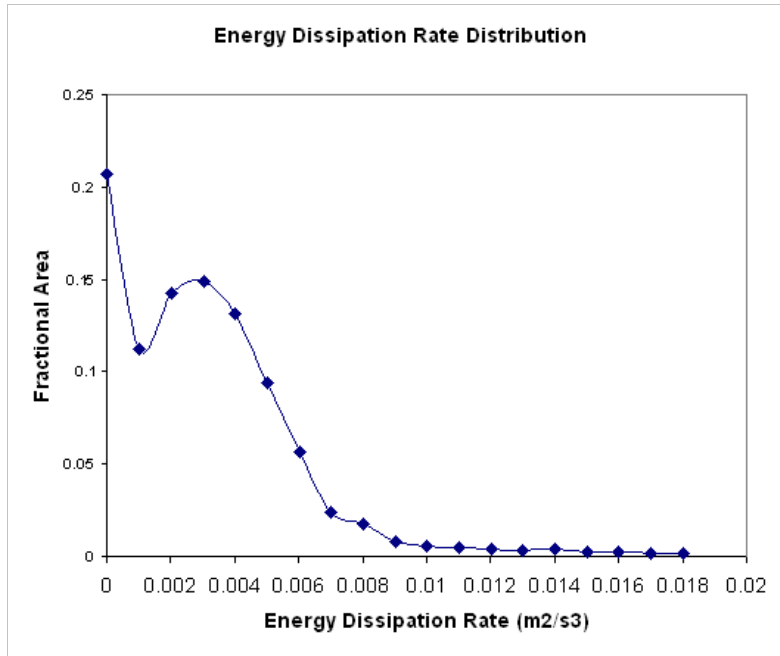
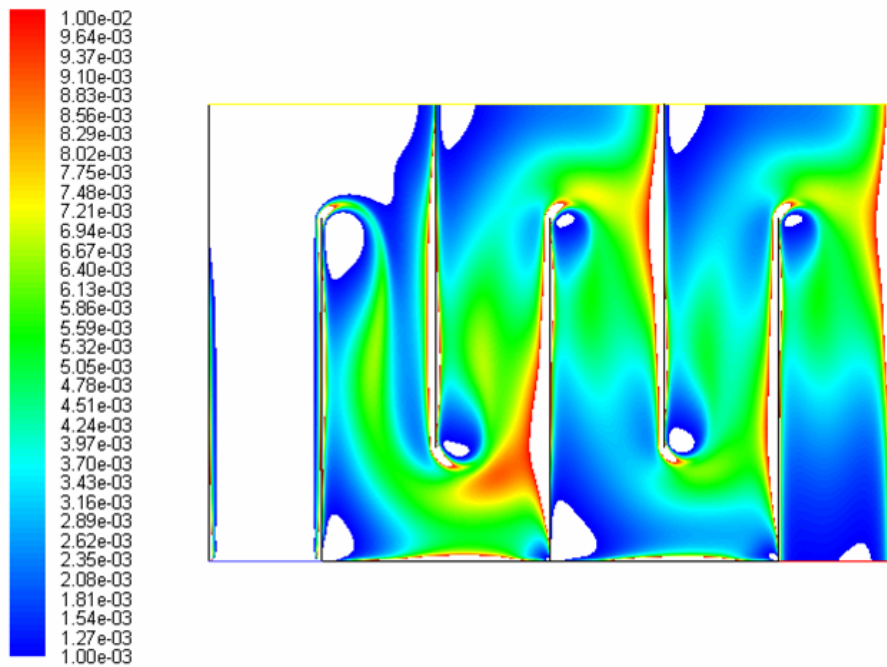


Figure III.10. Distribution of Energy Dissipation Rate ( $h/b=4$ ) with "hump"



Contours of Turbulent Dissipation Rate (Epsilon) (m<sup>2</sup>/s<sup>3</sup>)

Nov 24, 2008  
 FLUENT 6.3 (2d, dp, pbns, rke)

Figure III.11. Contour of Energy Dissipation Rate ( $h/b=4$ )

Figure III.10 shows the distribution of energy dissipation rate for flocculation tank height of 4b. We also see a visible hump. Figure III.11 shows the uniformity of energy dissipation rate with flocculation tank height of 4b.

Since hump appears both in the flocculation tank with uniform energy dissipation rate, we concluded that hump in the distribution of energy dissipation rate provided by UDF will be a good indication of uniformity.

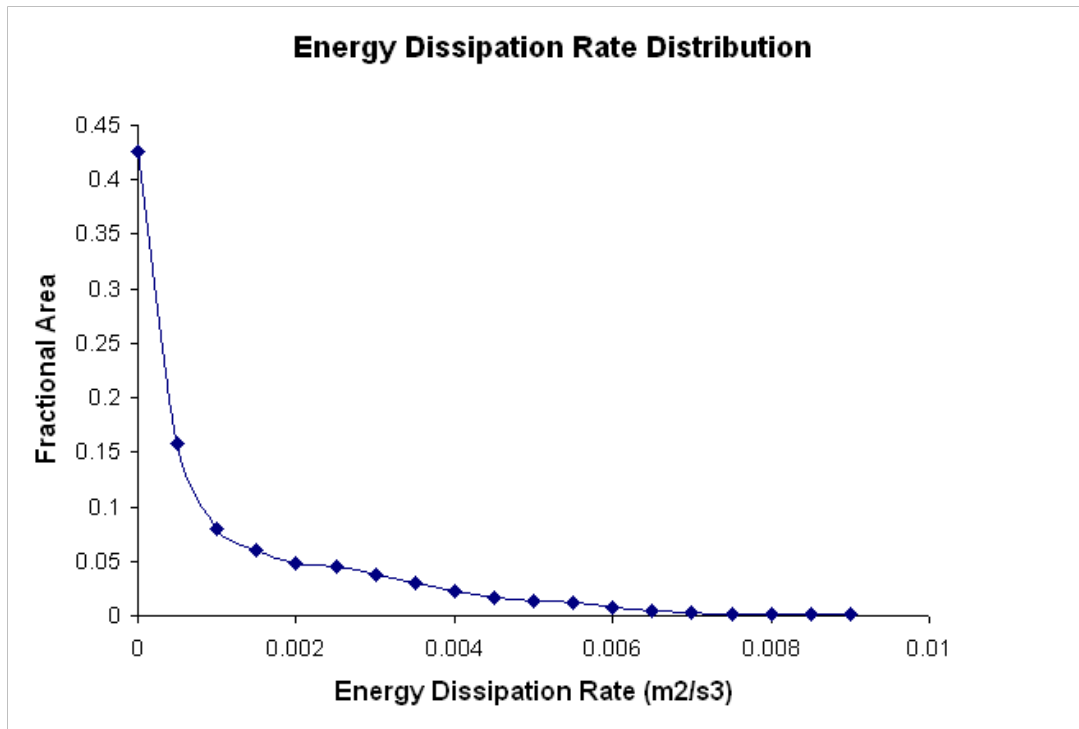
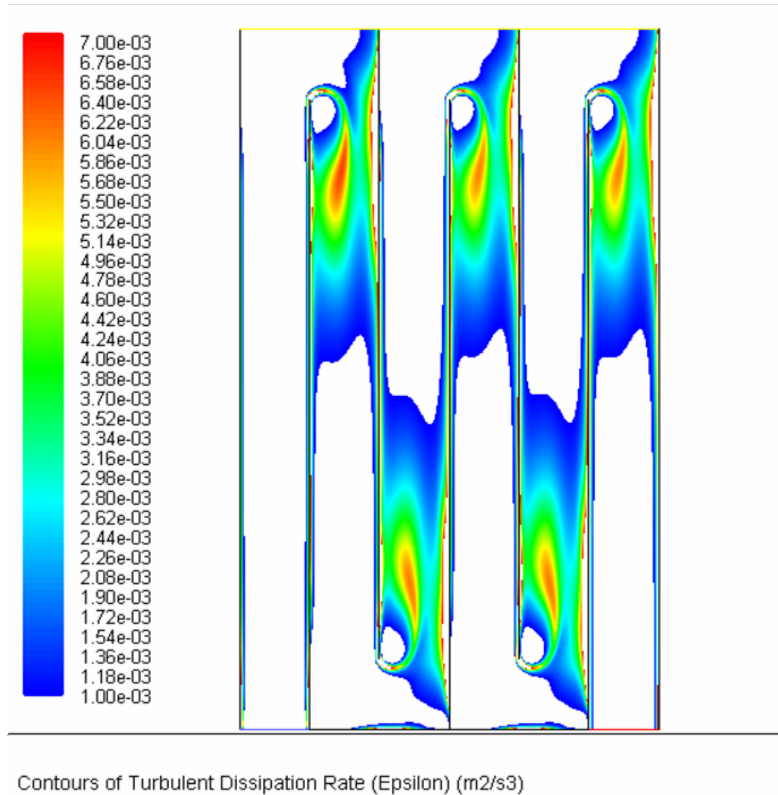


**Figure III.12. Distribution of Energy Dissipation Rate ( $h/b=10$ )**

For flocculation tank height of 10b, we see that there is no visible hump. From previous analysis, this indicates that the energy dissipation rate in the flocculation tank is not uniform.



Fl

**Figure III.13. Contour of Energy Dissipation Rate (h/b=10)**

Figure III.13 clearly shows the non-uniformity in energy dissipation rate for such geometry.

### **Result 3.3 - Performance Parameter Approach in Determining Optimal Geometry**

To determine the optimal geometry, performance parameters,  $\varepsilon\theta$ ,  $\varepsilon^{(1/2)}\theta$ ,  $\varepsilon^{(1/3)}\theta$ ,  $K$ , and  $G\theta$ , have calculated for each baffle for flocculation tank heights of .2, .3, .5, and 1. These performance parameters are extracted from the results of the converged solutions for the geometries listed above using the [UDF](#) shown in Appendix B-2.

**Table III.1 Summarized Data of Performance Parameters**

Flocculation Tank Height (H/w) of 2						
	B0	B1	B2	B3	B4	B5
$\Sigma \varepsilon \theta$	0.000037685	6.79E-05	0.000312	0.000545	0.000436	0.000496
K_baf_calc	0.7537	1.3586	6.2377	10.89996	8.72276	9.92732
K_baf_obs	0.7	4.7	8.8	6.3	7.2	7.1
$\Sigma \varepsilon^{1/2} \theta$	0.000354	0.000645	0.002006	0.002753	0.002478	0.002719
$\Sigma \varepsilon^{1/3} \theta$	0.0012259	0.001885	0.004202	0.005167	0.004849	0.005178
$\pi$ -cell	0.69919499	0.99297	1.542364	1.590964	1.616837	<b>1.672407</b>
G $\theta$	35.34701918	64.42344	200.3287	274.9119	247.3952	271.4571
G $\theta m^2$						9115.529

Flocculation Tank Height (H/w) of 3						
	B0	B1	B2	B3	B4	B5
$\Sigma \varepsilon \theta$	3.6508E-05	0.00017	0.000393	0.000364	0.000298	0.000312
K_baf_calc	0.730168	3.4036	7.86976	7.27116	5.96102	6.24676
K_baf_obs	0.3	5.1	6.6	5.7	5.3	4.8
$\Sigma \varepsilon^{1/2} \theta$	0.0521187	0.166315	0.29563	0.288476	0.259631	0.270448
$\Sigma \varepsilon^{1/3} \theta$	0.00180651	0.004152	0.00627	0.006175	0.005764	0.005929
$\pi$ -cell	1.27076181	2.050469	2.503142	2.544591	2.534492	<b>2.582916</b>
G $\theta$	52.0406974	166.0661	295.1876	288.0443	259.2424	270.0432
G $\theta m^2$						7392.357

Flocculation Tank Height (H/w) of 5						
	B0	B1	B2	B3	B4	B5
$\Sigma \varepsilon \theta$	5.02E-05	0.000227	0.000253	0.00023	0.000232	0.000225
K_baf_calc	1.003114	4.53988	5.05864	4.59934	4.63584	4.49742
K_baf_obs	0.4	4.1	3.9	3.7	3.9	4
$\Sigma \varepsilon^{1/2} \theta$	0.085273	0.270593	0.297324	0.281896	0.283379	0.281935
$\Sigma \varepsilon^{1/3} \theta$	0.002973	0.006925	0.007425	0.007169	0.007195	0.007175
$\pi$ -cell	2.288513	3.824623	4.022941	4.00287	4.008508	<b>4.052818</b>
G $\theta$	85.14498	270.188	296.879	281.4741	282.9549	281.513
G $\theta m^2$						4993.847

Flocculation Tank Height (H/w) of 10						
	B0	B1	B2	B3	B4	B5
$\Sigma \varepsilon \theta$	7.68E-05	0.000274	0.000264	0.000266	0.000265	0.000261
K_baf_calc	1.5368	5.48	5.286	5.326	5.298	5.216
K_baf_obs	0.5	4.55	4.26	4.2	4.01	4.76
$\Sigma \varepsilon^{1/2} \theta$	0.1522	0.391	0.3868	0.3871	0.3876	0.3874
$\Sigma \varepsilon^{1/3} \theta$	0.005243	0.010933	0.01088	0.010871	0.010898	0.010872
$\pi$ -cell	4.33088	6.906114	6.980632	6.945742	6.990033	<b>7.01918</b>
G $\theta$	151.9722	390.4148	386.2211	386.5207	387.0199	386.8202
G $\theta m^2$						3481.615

\*Note that eps\_1/2 values for H/w of 3,5,10 are normalized by the flow (x100).

## Performance Based Analysis

From the data, observations about the values of the performance parameters can be made:

- The  $G\theta/m^2$  value decreases with increasing flocculation tank height indicating that the most efficient flocculation occurs at a  $h/w$  ratio of 2. This type of trend would be exhibited for  $\epsilon\theta$ ,  $\epsilon^{(1/2)}\theta$ , and  $\epsilon^{(1/3)}\theta$  if they were normalized by area.
- Similarly, larger pressured drops,  $K$  for both observed and calculated are exhibited for flocculation tank with smaller heights. This reflects how energy dissipation regions intersect with each other.
- Large flocculation tank heights have a more uniform performance over all baffles, and reach a converged baffle solution more quickly than the smaller flocculation tank heights.

## Pi Cell Analysis

The region of high energy dissipation behind a baffle can be categorized by estimating by pi cell value (the length of the region in terms of the width in between baffles). Interestingly with larger flocculation tank heights the pi-cell values bolded in the charts above continue to increase.

From observations of the energy dissipation regions in tall ( $h/w > 5$ ) flocculation tanks, the energy dissipation regions do not interact with the separation region at the subsequent region. Thus, it seems reasonable to conclude that there is a maximum pi-cell value that would be constant with increasing pi-cell values. However, in the formulation of this quantity, the energy dissipation from the entire baffle is summed (including energy dissipation from the walls), and thus the increasing flocculation tank heights results in increasing pi-cell values.

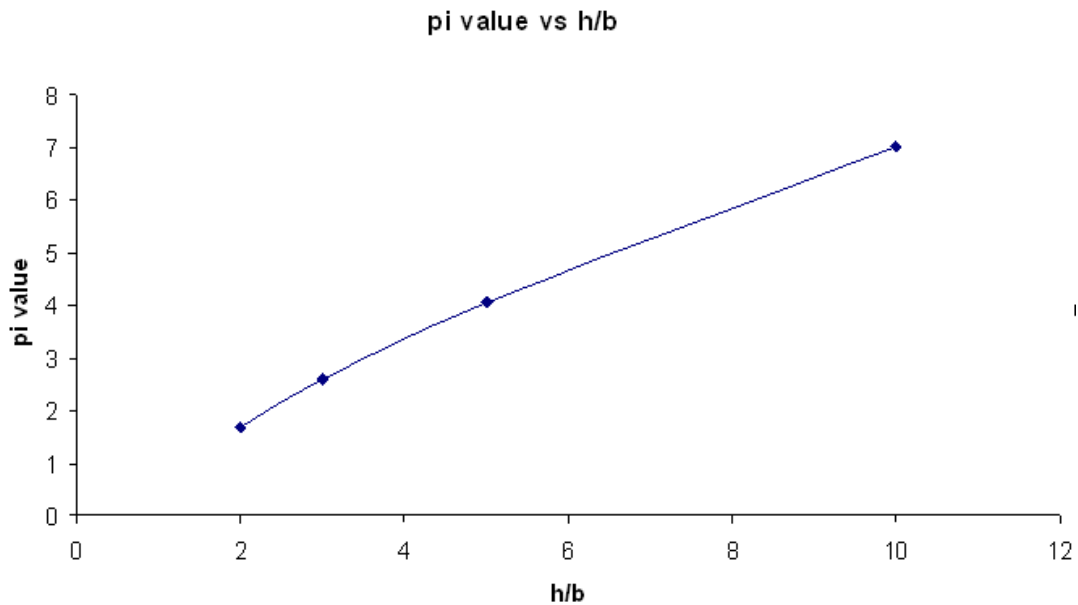


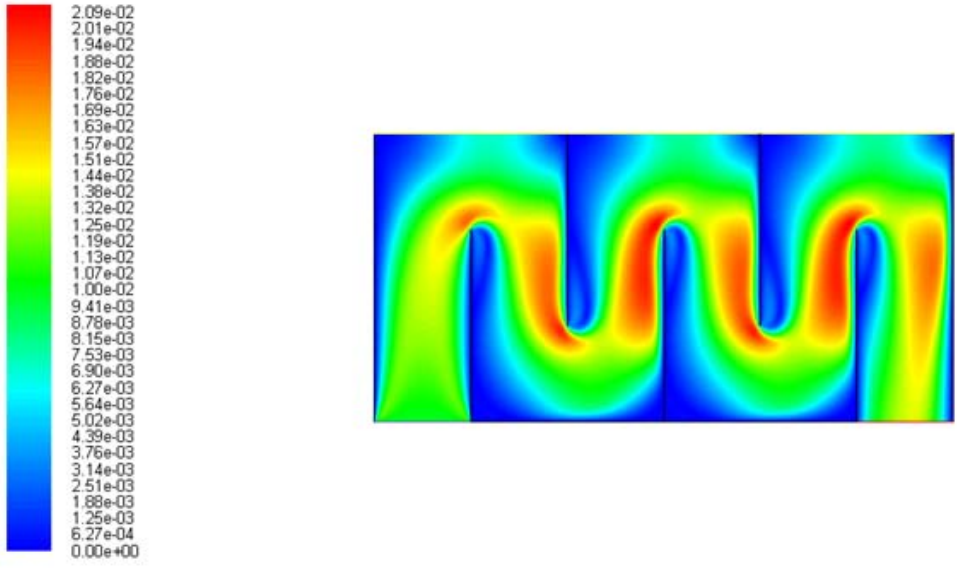
**Figure III.14. pi-cell values as a function of the height**

### **Discussion 3.1 Sensitivity to Reynolds Number**

A sensitivity analysis of Reynolds number for the flocculation height tank height of .3 with a symmetry boundary condition has been completed. The performance of the flocculator was examined at  $Re=1,000$  (corresponding to a velocity inlet of .01 m/s),  $Re=10,000$  (velocity inlet of .1 m/s), and  $Re=100,000$  (velocity inlet of 1 m/s).

#### **Velocity Profiles**

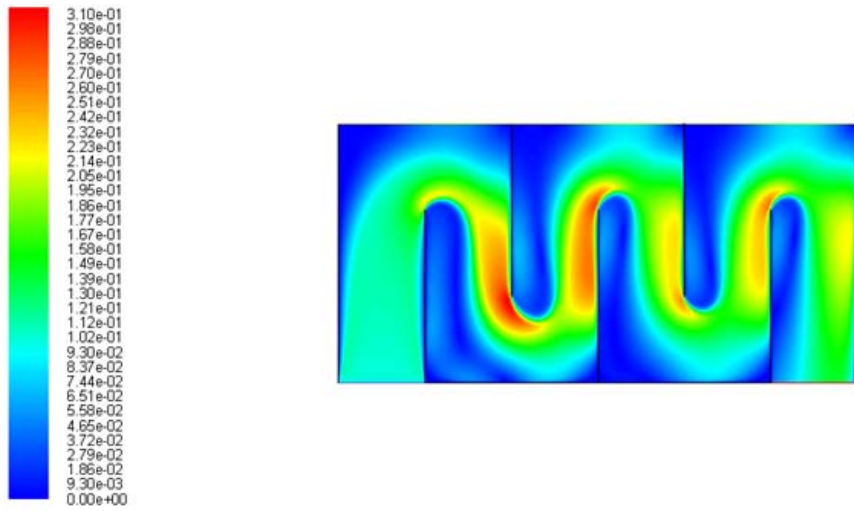
The velocity profiles for varying Reynolds numbers are presented below. With increasing inlet velocities, the uniformity of the flow decreases. This can be seen by how the ratio of the maximum velocity over the inlet velocity increases, as well by the color contour velocity profiles.



Contours of Velocity Magnitude (m/s)

Dec 08, 2008  
FLUENT 6.3 (2d, dp, pbns, rke)

**Figure III.15. Velocity inlet = .01 m/s (Re=1,000)**



Contours of Velocity Magnitude (m/s)

Dec 08, 2008  
FLUENT 6.3 (2d, dp, pbns, rke)

**Figure III.16. Velocity inlet = .1 m/s (Re=10,000)**

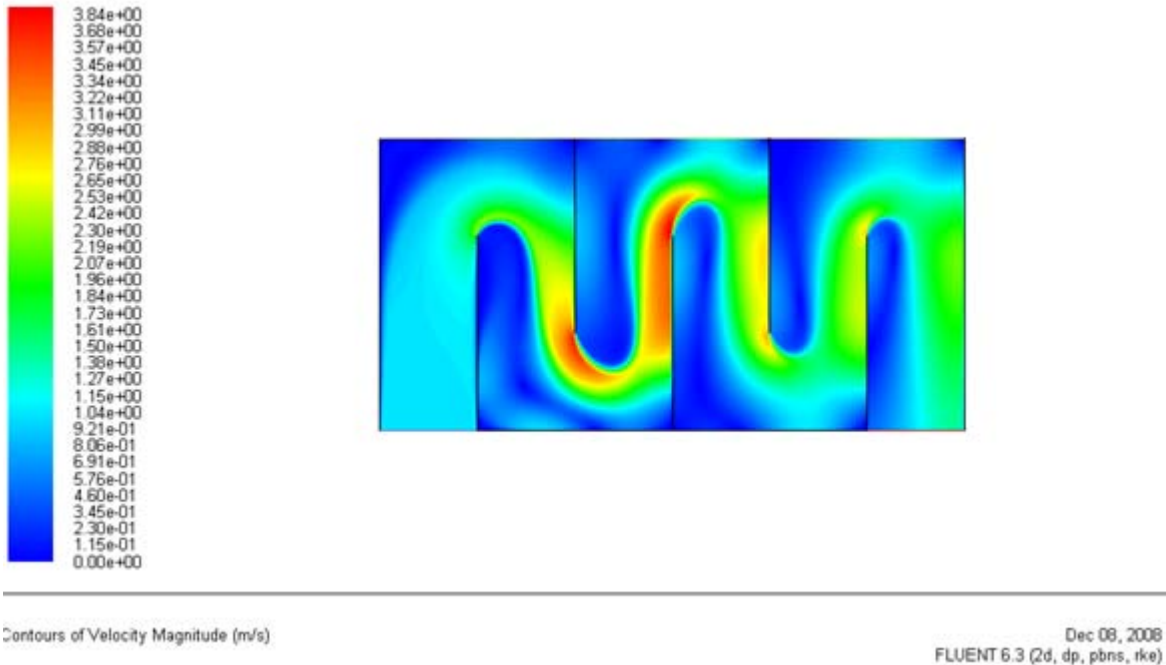


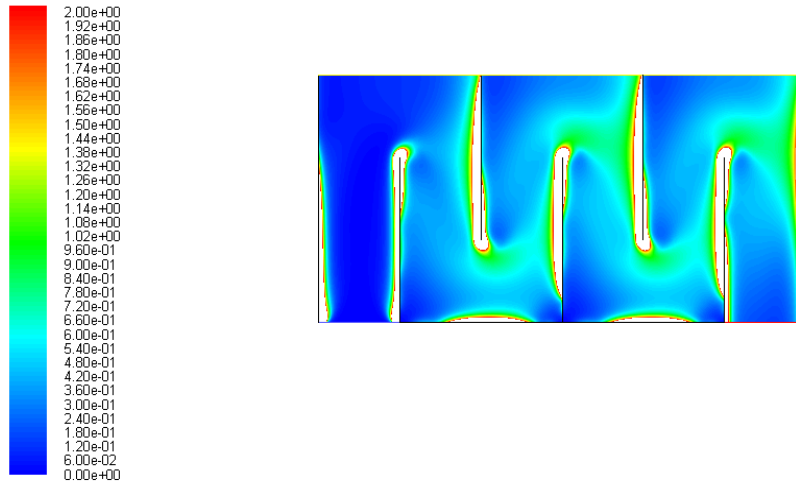
**Figure III.17. Velocity inlet = 1 m/s (Re=100,000)**

For the case when the Reynolds number is 1,000, the flow is in the laminar region, and the fluid behaves similarly across different baffles. The velocity profile, which has a maximum magnitude of only twice the inlet value, reveals that the recirculating region is smaller, and the fluid does not impinge on the baffle following it. The velocity profile of the Re=100,000 case shows that the fluid does not have a high enough viscosity to turn around the bends efficiently. After each turn the fluid impinges upon the baffle following it. The flow over the first baffle channels the fluid creating an extremely high velocity region at the edge of the second baffle. Following this baffle there is an extremely high region of velocity correspond to how a lot of fluid is forced against the edge of the third baffle.

### Normalized Energy Dissipation Profiles

The normalized energy dissipation for varying Reynolds Numbers is presented below. With increasing Reynolds numbers, the energy dissipation profile reveals a greater amount of energy dissipation in areas where the fluid impinges on the following baffle.

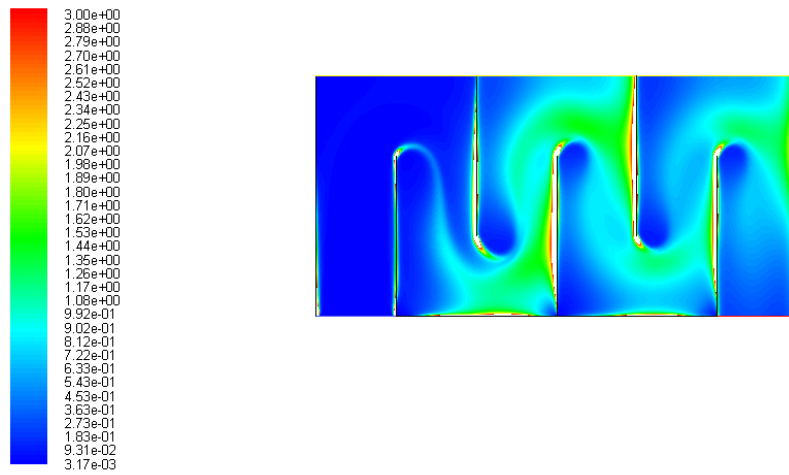




Contours of custom-function-0

Dec 11, 2008  
FLUENT 6.3 (2d, dp, pbns, rke)

**Figure III.18. Normalized Epsilon Values for Velocity inlet = .01 m/s (Re=1,000)**



Contours of custom-function-0

Dec 11, 2008  
FLUENT 6.3 (2d, dp, pbns, rke)

**Figure III.19. Normalized Epsilon Values for Velocity inlet = . 1 m/s (Re=10,000)**

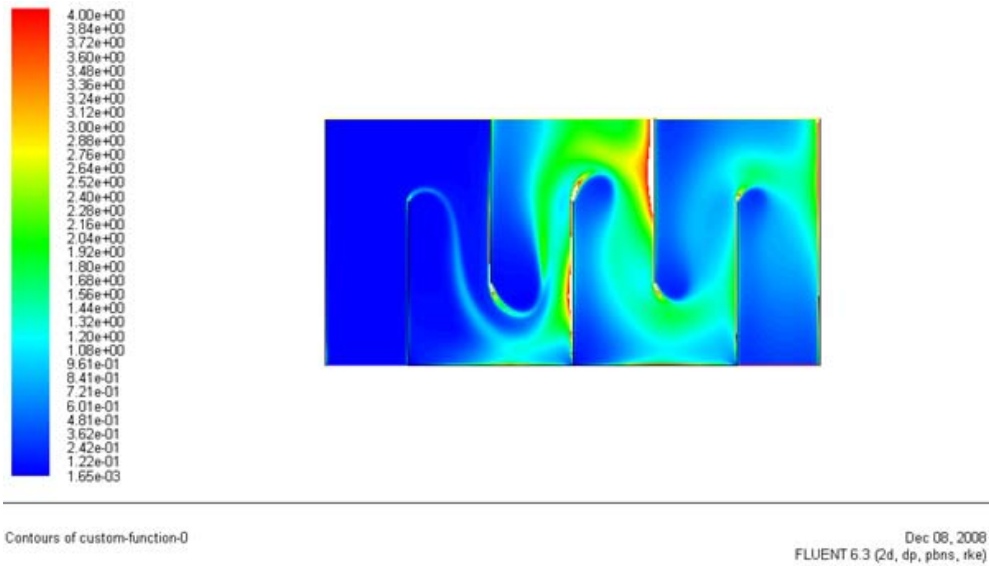


**Figure III.20. Normalized Epsilon Values for Velocity inlet = 1 m/s (Re=100,000)**

The normalized energy dissipation profile in Figure 4 for Re=1,000 reveals that the fluid only dissipates energy due to the no slip conditions on the wall. Otherwise, the energy dissipation is quite boring, and there is little energy dissipation induced in the main portion of the flow of the fluid, even after the baffles. In the higher Reynolds values the normalized dissipation values increase, and higher spikes occur where the fluids impinges upon the next baffle. There is a slight difference in the profiles of the Re=10,000 and 100,000 cases. The Re=100,000 flow does not make use of the space of the flocculation tank as efficiently as the Re=10,000 flow, and the dissipation regions are more pinched. This is reflected by the higher angle of separation at the baffle, and less uniformity.

**Performance Parameters for Re=100,000**

Below is the performance parameters for the tank with Re=100,000 for baffles 1-6.

Flocculation Tank Height (H/w) of 3, Re= 100,000						
$\sum \epsilon \theta$	0.006012	0.056728	0.338136	0.470983	0.289111	0.281172
$\sum \epsilon^{1/2} \theta$	0.009341	0.032178	0.091802	0.110472	0.088998	0.087063
pi-cell (K_c)	1.933081	2.144314	2.639679	2.720154	2.824559	2.797107
pi-cell (K_o)	0.947922	1.070769	3.325883	4.073676	3.391765	3.040231
π-cell	1.933081	2.144314	2.639679	2.720154	2.824559	<b>2.797107</b>
Gθ	93.2699	321.2934	916.6421	1103.067	888.644	869.33
Gθ/m <sup>2</sup>						27948.31

The performance parameters reflects that the higher energy dissipation results in a flocculation tank design with a higher pi-cell value and a higher Gθ value. However, clearly the spike in energy dissipation will cause flocs to break up, and not all of the flocculation tank is being effectively used.

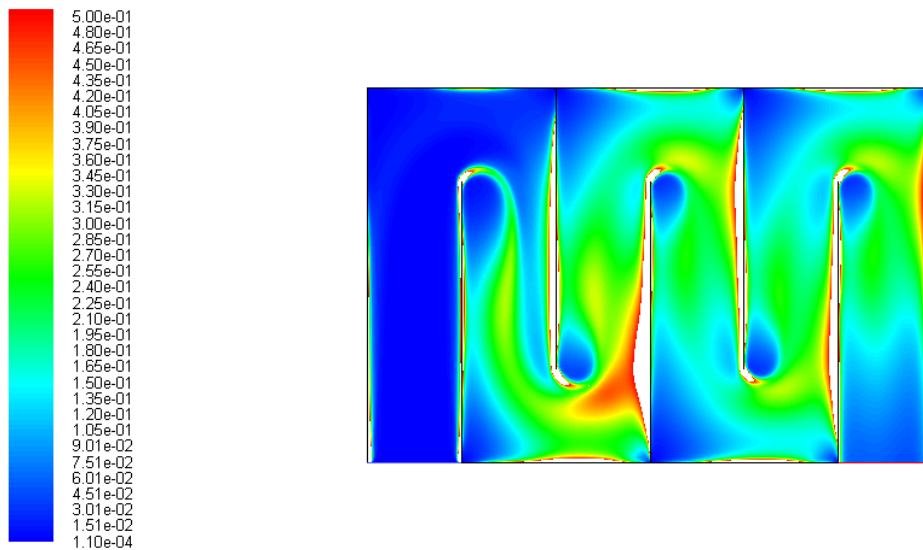
Overall, the sensitivity analysis has shown that the Reynolds number does impact the normalized epsilon value. However, a small adjustment in flow rate will not result in drastic changes in performance of the flocculation tank.

### Discussion 3.2: Nondimensional Analysis

Dimensional analysis relates  $\epsilon$  to  $K, V, \pi$  and baffle width, as follows:

$$\epsilon = KV^3 / (2*\pi\text{-cell}*b)$$

Thus,  $\epsilon*b/V^3$  represents a dimensionless quantity where  $K$  is the minor loss coefficient (the drop in the pressure coefficient per baffle),  $b$  is the baffle spacing, and  $V$  is the average velocity flowing through the channel when the baffle spacing is  $b$ . Throughout this research paper, dimensionless epsilon was used to compare flow with different geometric and flow properties to ensure accurate comparison.



Contours of nondimepsilon

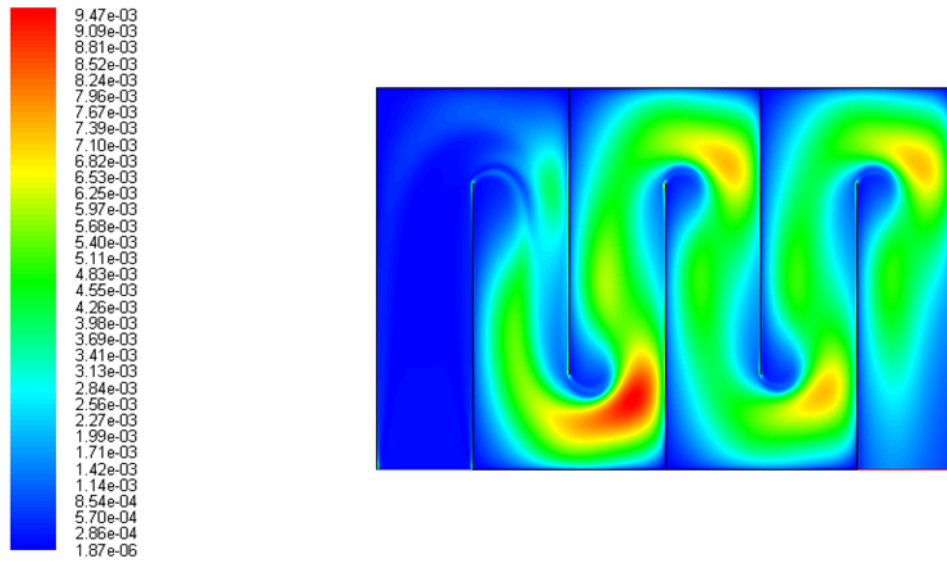
Nov 05, 2008  
FLUENT 6.3 (2d, dp, pbns, rke)

**Figure III.21. Nondimensionalized energy dissipation rate (fh = 0.4 bs = 0.1, v = 0.1)**

Figure III.21 shows an example of nondimensionalized contour of energy dissipation rate. Note that for above example, the nondimensionalized epsilon differs by a factor of 100 compared to the epsilon.

### Discussion 3.3 Investigation of Turbulence Boundary Condition

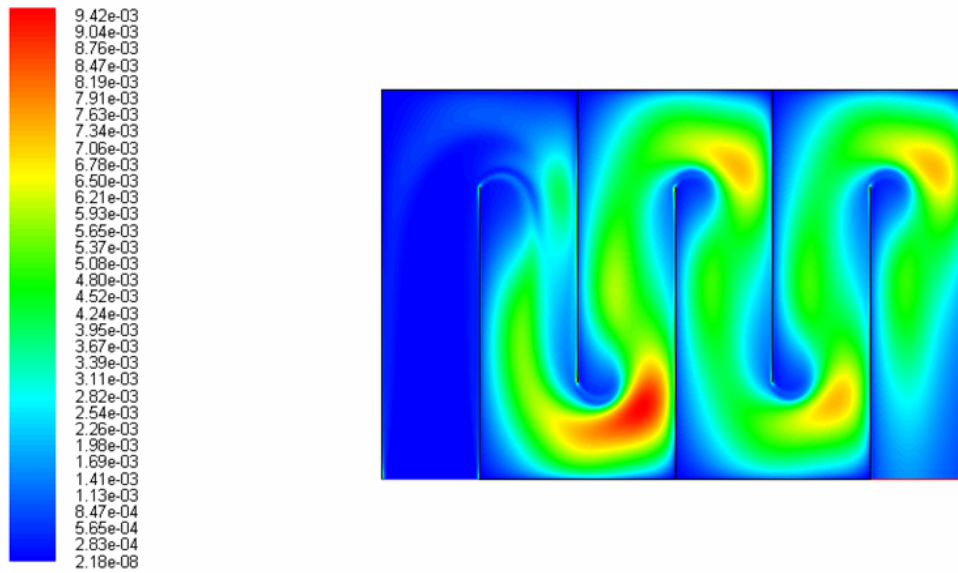
The effect of turbulence boundary condition has been examined by varying the inlet condition. The following three plots of energy dissipation illustrate the result.



Contours of Turbulent Kinetic Energy (k) (m<sup>2</sup>/s<sup>2</sup>)

Oct 30, 2008  
FLUENT 6.3 (2d, dp, pbns, rke)

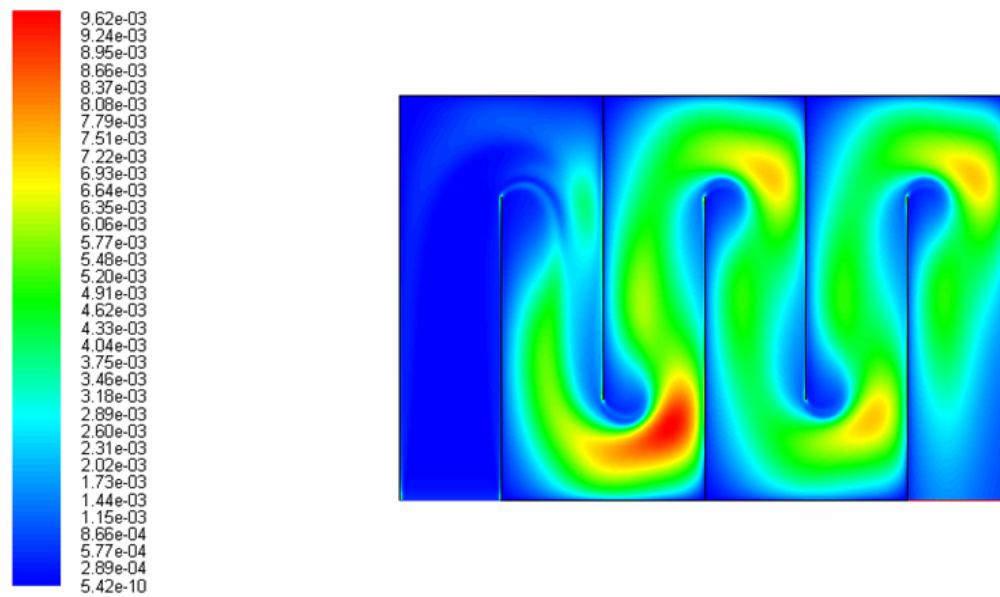
**Figure III.22. Turbulent intensity 10% Turbulent length scale 0.004 (BL thickness \* 0.4)**



Contours of Turbulent Kinetic Energy (k) (m2/s2)

Oct 30, 2008  
FLUENT 6.3 (2d, dp, pbns, rke)

**Figure III.23. Turbulent intensity 1% Turbulent length scale 0.04**



Contours of Turbulent Kinetic Energy (k) (m2/s2)

Oct 30, 2008  
FLUENT 6.3 (2d, dp, pbns, rke)

**Figure III.24. Turbulent Intensity 20% Turbulent length scale 0.0004**

Comparing figure III.22, III.23 and III.24, large changes of turbulence boundary conditions does not significantly affect the solution. Final boundary condition is the Turbulent intensity of 10% and turbulent length scale of 0.004, which is approximately .4\*boundary layer thickness.

### Discussion 3.4 Validation of Results

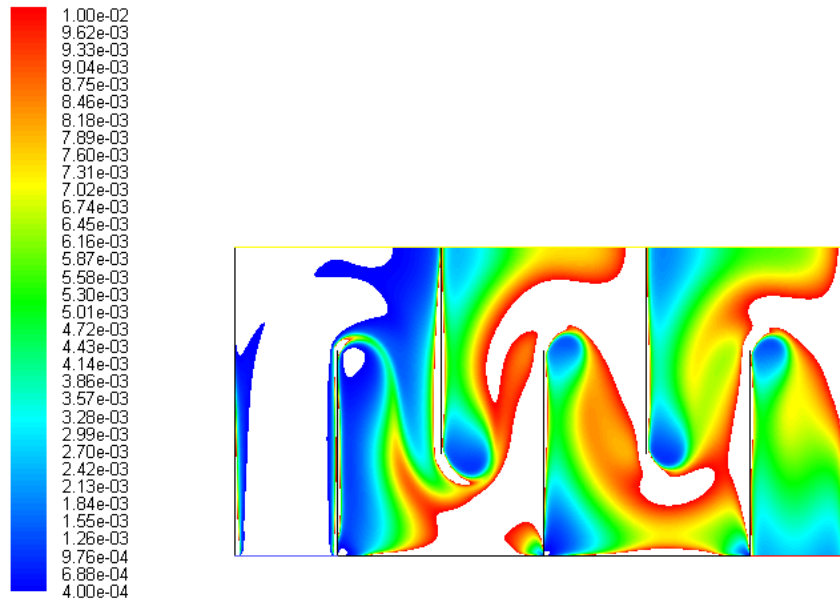
It is important to confirm that the results generated by FLUENT are comparable to values from literature. For flocculators without recirculating solids, the recommended  $G\theta$  is between 20,000-150,000 (Schulz, C. R. and D. A. Okun. Surface Water Treatment for Communities in Developing Countries, John Wiley & Sons. 1984). The results from FLUENT normalized by the flocculation area are shown below in Table III.2:

**TABLE III.2.  $G\theta$  normalized by area for different geometries**

Case Geometry (h-height,b-width,N-baffles)	$G\theta$ Flocculator/ $m^2$
b=.1, h=1, N=1, Clearance height=.15	4,300
b=.1, h=.3, N=5, sym bc	8,870
b=.1, h=.2, N=5	10,600

Dividing the recommended  $G\theta$  value by the normalized values, estimates the area required by the flocculation tank. This corresponds to 2-15  $m^2$  of flocculator area based on the weighted  $G\theta$ -values calculated. The area of flocculators currently used in practice in Honduras is within this range. Thus, the calculated  $G\theta$ -values seem sensible.

Another check of the accuracy of the results can be seen by comparing the dissipation rate of the flocculation tanks to values recommended by Schulz and Okun of .4-10 mW/kg. The energy dissipation plotted in this region for the fh=3 case results in the plot shown below:



Contours of Turbulent Dissipation Rate (Epsilon) (m2/s3)

Dec 09, 2008  
FLUENT 6.3 (2d, dp, pbns, rke)

**Figure III.25. Energy Dissipation Rate in the range of .4-10 mW/kg for fh/w=3, Re=10,000**

The regions in white are outside of this region, indicating that energy dissipation values above and below this recommended region exist in the flocculation tank. Note that after the first baffle, very little of the fluid is below the recommended energy, and the white regions are high turbulent kinetic energy dissipation areas.

## IV. Conclusion

K-ε realizable turbulence model is suitable for modeling the flow in the flocculation tank. Result of the modeling is insensitive to the turbulence boundary condition used. Result of the modeling is sensitive to the Reynolds number.

Two design approaches can be utilized to find the optimal geometry for flocculation tank. The first approach is to analyze the uniformity of energy dissipation rate contour. The second approach is to analyze the performance parameters such as  $\epsilon\theta$ ,  $\epsilon^{1/2}\theta$ ,  $\epsilon^{1/3}\theta$ , and  $G\theta$ .

Using first approach, it is concluded that for a flow of  $Re = 10,000$ , the optimal geometry is  $fh = 0.3m$ ,  $b = 0.1m$ ,  $ch = 0.1m$ . Using the second approach, it is concluded that for a flow of  $Re = 10,000$ , the optimal geometry is  $fh = 0.2m$ ,  $b = 0.1m$ ,  $ch = 0.1m$ .

Both approaches suggest that smaller flocculation tank height with intersecting energy dissipation regions will produce a better performing flocculation tank.

## Appendix A-1: Gambit Automation Script

```
/ Journal File for GAMBIT 2.4.6, Database 2.4.4, ntx86 SP2007051421
/ Identifier "Clean Script"
/ File opened for write Wed Oct 08 09:16:13 2008.
undo begingroup

/clearance height
$ch = 0.1

/flocculator height
$fh = 0.5

/create baffle spacing
$bs1 = 0.1
$bs2 = 0.1
$bs3 = 0.1
$bs4 = 0.1
$bs5 = 0.1
$bs6 = 0.1

/create x-coordinate
$w0 = 0
$b1 = $w0+$bs1
$b2 = $b1+$bs2
$b3 = $b2+$bs3
$b4 = $b3+$bs4
$b5 = $b4+$bs5
$w6 = $b5+$bs6

/create y-coordinate
$y1 = $ch
$y2 = $fh-$ch

coordinate modify "c_sys.1" xyplane xaxis add 0 AND 0.1 reset snap lines
coordinate modify "c_sys.1" xyplane yaxis add 0 AND 0.1 reset snap lines
window modify coordinates "c_sys.1" xyplane grid
undo endgroup
undo begingroup
coordinate modify "c_sys.1" xyplane xaxis add 0 AND 0.1 reset snap lines
coordinate modify "c_sys.1" xyplane yaxis reset snap lines
window modify coordinates "c_sys.1" xyplane grid
undo endgroup
undo begingroup
coordinate modify "c_sys.1" xyplane xaxis add 0 AND 0.1 AND 0.2 AND 0.3 AND \
0.4 AND 0.5 AND 0.6 reset snap lines
```



```
coordinate modify "c_sys.1" xyplane yaxis reset snap lines
window modify coordinates "c_sys.1" xyplane grid
undo endgroup
undo begingroup
coordinate modify "c_sys.1" xyplane xaxis add 0 AND 0.1 AND 0.2 AND 0.3 AND \
  0.4 AND 0.5 AND 0.6 reset snap lines
coordinate modify "c_sys.1" xyplane yaxis add 0 AND 0.1 AND 0.2 AND 0.3 reset \
  snap lines
window modify coordinates "c_sys.1" xyplane grid
undo endgroup
vertex create coordinates 0 0 0
vertex create coordinates 0 $y1 0
vertex create coordinates 0 $y2 0
vertex create coordinates 0 $fh 0
vertex create coordinates $b1 0 0
vertex create coordinates $b1 $y1 0
vertex create coordinates $b1 $y2 0
vertex create coordinates $b1 $fh 0
vertex create coordinates $b2 0 0
vertex create coordinates $b2 $y1 0
vertex create coordinates $b2 $y2 0
vertex create coordinates $b2 $fh 0
vertex create coordinates $b3 0 0
vertex create coordinates $b3 $y1 0
vertex create coordinates $b3 $y2 0
vertex create coordinates $b3 $fh 0
vertex create coordinates $b4 0 0
vertex create coordinates $b4 $y1 0
vertex create coordinates $b4 $y2 0
vertex create coordinates $b4 $fh 0
vertex create coordinates $b5 0 0
vertex create coordinates $b5 $y1 0
vertex create coordinates $b5 $y2 0
vertex create coordinates $b5 $fh 0
vertex create coordinates $w6 0 0
vertex create coordinates $w6 $y1 0
vertex create coordinates $w6 $y2 0
vertex create coordinates $w6 $fh 0
```

```
edge create straight "vertex.1" "vertex.2" "vertex.3" "vertex.4"
edge create straight "vertex.5" "vertex.6" "vertex.7" "vertex.8"
edge create straight "vertex.9" "vertex.10" "vertex.11" "vertex.12"
edge create straight "vertex.13" "vertex.14" "vertex.15" "vertex.16"
edge create straight "vertex.17" "vertex.18" "vertex.19" "vertex.20"
edge create straight "vertex.21" "vertex.22" "vertex.23" "vertex.24"
edge create straight "vertex.25" "vertex.26" "vertex.27" "vertex.28"
```

```

edge create straight "vertex.4" "vertex.8" "vertex.12" "vertex.16" \
"vertex.20" "vertex.24" "vertex.28"
edge create straight "vertex.3" "vertex.7" "vertex.11" "vertex.15" \
"vertex.19" "vertex.23" "vertex.27"
edge create straight "vertex.2" "vertex.6" "vertex.10" "vertex.14" \
"vertex.18" "vertex.22" "vertex.26"
edge create straight "vertex.1" "vertex.5" "vertex.9" "vertex.13" "vertex.17" \
"vertex.21" "vertex.25"
/ERROR occurred in the next command!
face create wireframe "edge.1" "edge.2" "edge.3" "edge.4" "edge.5" "edge.6" \
"edge.7" "edge.8" "edge.9" "edge.10" "edge.11" "edge.12" "edge.13" \
"edge.14" "edge.15" "edge.16" "edge.17" "edge.18" "edge.19" "edge.20" \
"edge.21" "edge.22" "edge.23" "edge.24" "edge.25" "edge.26" "edge.27" \
"edge.28" "edge.29" "edge.30" "edge.31" "edge.32" "edge.33" "edge.34" \
"edge.35" "edge.36" "edge.37" "edge.38" "edge.39" "edge.40" "edge.41" \
"edge.42" "edge.43" "edge.44" "edge.45" real
face create wireframe "edge.3" "edge.22" "edge.6" "edge.28" real
face create wireframe "edge.2" "edge.5" "edge.34" "edge.28" real
face create wireframe "edge.1" "edge.34" "edge.4" "edge.40" real
undo begingroup
coordinate modify "c_sys.1" xyplane xaxis add 0 AND 0.1 AND 0.2 AND 0.3 AND \
0.4 AND 0.5 AND 0.6 reset snap lines
coordinate modify "c_sys.1" xyplane yaxis add 0 AND 0.1 AND 0.2 AND 0.3 reset \
snap lines
window modify coordinates "c_sys.1" xyplane nogrid
undo endgroup
face create wireframe "edge.23" "edge.9" "edge.29" "edge.6" real
face create wireframe "edge.29" "edge.8" "edge.35" "edge.5" real
face create wireframe "edge.35" "edge.7" "edge.41" "edge.4" real
face create wireframe "edge.24" "edge.12" "edge.30" "edge.9" real
face create wireframe "edge.30" "edge.11" "edge.36" "edge.8" real
face create wireframe "edge.36" "edge.10" "edge.42" "edge.7" real
face create wireframe "edge.25" "edge.15" "edge.31" "edge.12" real
face create wireframe "edge.31" "edge.14" "edge.37" "edge.11" real
face create wireframe "edge.37" "edge.13" "edge.43" "edge.10" real
face create wireframe "edge.26" "edge.18" "edge.32" "edge.15" real
face create wireframe "edge.32" "edge.17" "edge.38" "edge.14" real
face create wireframe "edge.38" "edge.16" "edge.44" "edge.13" real
face create wireframe "edge.27" "edge.21" "edge.33" "edge.18" real
face create wireframe "edge.33" "edge.20" "edge.39" "edge.17" real
face create wireframe "edge.39" "edge.19" "edge.45" "edge.16" real
undo begingroup
blayer create first 0.001 growth 1.4 total 0.00436 rows 3 transition 1 \
trows 0 uniform
blayer attach "b_layer.1" face "face.2" "face.1" "face.3" "face.1" "face.1" \
"face.4" "face.2" "face.5" "face.3" "face.6" "face.3" "face.4" "face.4" \

```

```

"face.7" "face.5" "face.8" "face.6" "face.9" "face.6" "face.7" "face.7" \
"face.10" "face.8" "face.11" "face.9" "face.12" "face.9" "face.10" \
"face.10" "face.13" "face.11" "face.14" "face.12" "face.15" "face.12" \
"face.13" "face.13" "face.16" "face.14" "face.17" "face.15" "face.18" \
"face.15" "face.16" "face.16" "face.17" "face.18" "face.18" edge "edge.2" \
"edge.3" "edge.1" "edge.22" "edge.6" "edge.6" "edge.5" "edge.5" "edge.4" \
"edge.4" "edge.40" "edge.23" "edge.9" "edge.9" "edge.8" "edge.8" "edge.7" \
"edge.7" "edge.41" "edge.24" "edge.12" "edge.12" "edge.11" "edge.11" \
"edge.10" "edge.10" "edge.42" "edge.25" "edge.15" "edge.15" "edge.14" \
"edge.14" "edge.13" "edge.13" "edge.43" "edge.26" "edge.18" "edge.18" \
"edge.17" "edge.17" "edge.16" "edge.16" "edge.44" "edge.27" "edge.21" \
"edge.20" "edge.19" "edge.45" add
undo endgroup
undo begingroup
edge picklink "edge.45" "edge.44" "edge.43" "edge.42" "edge.41" "edge.40" \
"edge.39" "edge.38" "edge.37" "edge.36" "edge.35" "edge.34" "edge.33" \
"edge.32" "edge.31" "edge.30" "edge.29" "edge.28" "edge.27" "edge.26" \
"edge.25" "edge.24" "edge.23" "edge.22" "edge.21" "edge.20" "edge.19" \
"edge.18" "edge.17" "edge.16" "edge.15" "edge.14" "edge.13" "edge.12" \
"edge.11" "edge.10" "edge.9" "edge.8" "edge.7" "edge.6" "edge.5" "edge.4" \
"edge.3" "edge.2" "edge.1"
edge mesh "edge.1" "edge.2" "edge.3" "edge.4" "edge.5" "edge.6" "edge.7" \
"edge.8" "edge.9" "edge.10" "edge.11" "edge.12" "edge.13" "edge.14" \
"edge.15" "edge.16" "edge.17" "edge.18" "edge.19" "edge.20" "edge.21" \
"edge.22" "edge.23" "edge.24" "edge.25" "edge.26" "edge.27" "edge.28" \
"edge.29" "edge.30" "edge.31" "edge.32" "edge.33" "edge.34" "edge.35" \
"edge.36" "edge.37" "edge.38" "edge.39" "edge.40" "edge.41" "edge.42" \
"edge.43" "edge.44" "edge.45" successive ratio1 1 size 0.002
undo endgroup
face mesh "face.1" "face.2" "face.3" "face.4" "face.5" "face.6" "face.7" \
"face.8" "face.9" "face.10" "face.11" "face.12" "face.13" "face.14" \
"face.15" "face.16" "face.17" "face.18" map size 1
/ File opened for append Wed Oct 08 11:58:25 2008.
physics create "w0" btype "WALL" edge "edge.1" "edge.2" "edge.3"
physics create "b1" btype "WALL" edge "edge.5" "edge.4"
physics create "b2" btype "WALL" edge "edge.9" "edge.8"
physics create "b3" btype "WALL" edge "edge.10" "edge.11"
physics create "b4" btype "WALL" edge "edge.15" "edge.14"
physics create "b5" btype "WALL" edge "edge.17" "edge.16"
physics create "w6" btype "WALL" edge "edge.21" "edge.20" "edge.19"
physics create "top" btype "WALL" edge "edge.22" "edge.23" "edge.24" \
"edge.25" "edge.26" "edge.27"
physics create "bottom" btype "WALL" edge "edge.41" "edge.42" "edge.43" \
"edge.44"
physics create "Inlet" btype "VELOCITY_INLET" edge "edge.40"
physics create "Outlet" btype "PRESSURE_OUTLET" edge "edge.45"

```

## Appendix A-2: Fluent Automation Script

```
rc backstep_7800.cas y
define/models/viscous ke-realizable
yes
define models viscous near-wall-treatment enhanced-wall-treatment
no
define/materials change-create air
water
yes
boussinesq
998.2
no
no
yes
constant
0.001003
no
no
no
no
no
n
n
n
n
n
n
yes
define/operating-conditions operating-pressure
101325

//set bcs
//initialize

solve/set/equations flow
yes
solve/set/equations temperature
no
solve/set/equations ke
yes
solve/monitors/residual convergence-criteria
0.000001
0.000001
0.000001
0.000001
0.000001
```

```

solve/iterate
file/write-case "runkereal.cas"
define/models/viscous ke-realizable
solve iterate 1000
wcd "runkereal.cas"
exit

```

## Appendix B-1: UDF for Analyzing Distribution of Energy Dissipation Rate

```

/*****
  UDF to Look at the distribution of the energy dissipation rate
  *****/
/
#include "udf.h"

DEFINE_ON_DEMAND(on_demand_calc)
{
  Domain *d;

  real velocity;
  Thread *t;
  cell_t c;
  Node *nod;
  int n;
  double pos_x;
  double pos_y;
  double xvel;
  double yvel;
  double xprev=0;
  double yprev=0;
  double MeshArea=0;
  double cell_area=0;

  //bin analysis
  double checkmax = 0; // check max energy dissipation
  int binlength = 20;
  int binsize = 20;
  double bin[20]={0, 0, 0, 0, 0, 0, 0, 0, 0, 0, 0, 0, 0, 0, 0, 0, 0,
0, 0, 0};
  int i = 0;
  int j = 0;
  int nondimensionE = 1; // should be 100 if normalize
  double area[20]={0, 0, 0, 0, 0, 0, 0, 0, 0, 0, 0, 0, 0, 0, 0, 0, 0,
0, 0, 0};
  double start = 0.001;
  double end = 0.01;

  d = Get_Domain(1);      /* Get the domain using Fluent utility */

  /* Loop over all cell threads in the domain */
  thread_loop_c(t,d)
  {
    begin_c_loop(c,t)

```

```

{
    double delta_x = 0;
    double delta_y = 0;
    int run_number = 0;
    for (n=0; n < cell_type_nnodes[(int)C_TYPE(c,t)]; n++)
    {
        nod = C_NODE(c, t, n);
        pos_x=NODE_X(nod);
        pos_y=NODE_Y(nod);

        if(run_number>0)
        {
            if(delta_x<fabs(pos_x-xprev))
            delta_x= fabs(pos_x-xprev);

            if(delta_y < fabs(pos_y-yprev))
            delta_y = fabs(pos_y-yprev);

        }
        run_number = run_number +1;
        xprev = pos_x;
        yprev = pos_y;

    }
    MeshArea = MeshArea+delta_x*delta_y;
}
end_c_loop(c,t)
printf("\nMeshArea = %g\n", MeshArea);
/* Loop over all cells */
begin_c_loop(c,t)
{
    double delta_x = 0;
    double delta_y = 0;
    int run_number = 0;
    for (n=0; n < cell_type_nnodes[(int)C_TYPE(c,t)]; n++)
    {
        nod = C_NODE(c, t, n);
        pos_x=NODE_X(nod);
        pos_y=NODE_Y(nod);

        if(run_number>0)
        {
            if(delta_x<fabs(pos_x-xprev))
            delta_x= fabs(pos_x-xprev);

            if(delta_y < fabs(pos_y-yprev))
            delta_y = fabs(pos_y-yprev);

        }
        run_number = run_number +1;
        xprev = pos_x;
        yprev = pos_y;

    }
}

```

```

}

end_c_loop(c,t)

        checkmax = end - start;
printf("\nmax e = %g\n\n", checkmax);

for (i = 0; i<=binsize-1; i++)
{
        bin[i] = start + checkmax/binlength*i;
}

//chaterizing bins by looping through bins

for (i=0; i<=binsize-1; i++)
{
        //printf("\n bin = %g\n", bin[i]);

begin_c_loop(c, t)
{
        if(bin[i]<C_D(c,t) && C_D(c,t)<bin[i+1] )
        {
                double delta_x = 0;
                double delta_y = 0;
                int run_number = 0;
for (n=0; n < cell_type_nnodes[(int)C_TYPE(c,t)]; n++)
        {
                nod = C_NODE(c, t, n);
                pos_x=NODE_X(nod);
                pos_y=NODE_Y(nod);

                if(run_number>0)
                {
                        if(delta_x<fabs(pos_x-xprev))
                                delta_x= fabs(pos_x-xprev);

                        if(delta_y < fabs(pos_y-yprev))
                                delta_y = fabs(pos_y-yprev);

                }
                run_number = run_number +1;
                xprev = pos_x;
                yprev = pos_y;

                area[i] = delta_x*delta_y+area[i];

        }

}

}

```

```

        }
        end_c_loop(c,t)

        area[i]=area[i]/2/MeshArea;
        //if (i<=19)
        //{printf("\n area = %g\n", area[i]);}
    }

printf("bin\n");
for (j=0; j<=binsize-1; j++)
{printf(" %g\n", bin[j]);}
printf("\n area\n");
for (j=0; j<=binsize-1; j++)
{printf(" %g\n", area[j]);}

    }

}

```

## Appendix B-2: UDF for Extracting Performance Parameters

```

#include "udf.h"

DEFINE_ON_DEMAND(on_demand2_calc)
{
    Domain *d;

    real velocity;
    Thread *t;
    cell_t c;
    Node *nod;
    int n;
    int j;
    int density=1000;
    double flow=.01;
    double fh=1;
    double bl_thick=.01;
    double visc=1e-6;
    double pos_x;
    double pos_y;
    double xvel;
    double yvel;
    double xprev=0;
    double yprev=0;
    double MeshArea=0;
    double cell_area=0;
    double magvel=0;
    double flowtot=0;
    double baffle[7] = {0, .1, .2, .3, .4, .5, .6};
    double Monroe_sum1[6]={0, 0, 0, 0, 0, 0};
    double Monroe_sum2[6]={0, 0, 0, 0, 0, 0};
    double Monroe_sum3[6]={0, 0, 0, 0, 0, 0};
    double Manroe[6] = {0, 0, 0, 0, 0, 0};
    double display2 =0;
    double display1 =0;
}

```



```

int counter=0;
int q=0;

d = Get_Domain(1);      /* Get the domain using Fluent utility */

/* Loop over all cell threads in the domain */
for (q = 0; q <=5; q++)
{
    thread_loop_c(t,d)
    {
        begin_c_loop(c,t)
        {
            double delta_x = 0;
            double xpos_ave = 0;
            double delta_y = 0;
            double ypos_ave =0;
            int run_number = 0;
            for (n=0; n < cell_type_nnodes[(int)C_TYPE(c,t)]; n++)

                {
                    nod = C_NODE(c, t, n);
                    pos_x=NODE_X(nod);
                    pos_y=NODE_Y(nod);

                    if(run_number>0)
                    {
                        if(delta_x<fabs(pos_x-xprev))
                        delta_x= fabs(pos_x-xprev);

xpos_ave=pos_x*.5+xprev*.5;

                        if(delta_y < fabs(pos_y-yprev))
                        delta_y = fabs(pos_y-yprev);

ypos_ave=pos_y*.5+yprev*.5;

                    }
                    run_number = run_number +1;
                    xprev = pos_x;
                    yprev = pos_y;

                }
            if(xpos_ave>(baffle[q]+bl_thick) &
xpos_ave<(baffle[q+1]-bl_thick) & ypos_ave>bl_thick & ypos_ave<(fh-
bl_thick))
            {
                Monroe[q]=Manroe[q]+delta_x*delta_y;
                Monroe_sum1[q] = Monroe_sum1[q] +
pow(C_D(c,t),.333)*delta_x*delta_y;
                Monroe_sum2[q] = Monroe_sum2[q] +
pow(C_D(c,t),0.5)*delta_x*delta_y;
                Monroe_sum3[q] = Monroe_sum3[q] +
C_D(c,t)*delta_x*delta_y;
            }
        }
        end_c_loop(c,t);
    }
}

```

```
}
    printf("Eps_onethird_pheta %g\n");
for (q=0; q<=5; q++)
    {printf("%g\n",Monroe_sum1[q]/flow);}
printf("Eps_onehalf_pheta = %g\n");
for (q=0; q<=5; q++)
    {printf("%g\n",Monroe_sum2[q]/flow);}
printf("Eps_one_pheta = %g\n");
for (q=0; q<=5; q++)
    printf("%g\n",Monroe_sum3[q]/flow);
for (q=0; q<=5; q++)
printf("Area = %g\n", Manroe[q]);
}
```